Studies on epidemiology and virus-host interaction in pathogenicity of Tick-borne encephalitis virus

（ダニ媒介性脳炎ウイルスの疫学および病原性発現に関与する宿主因子の研究）

2018

Memi Muto

Laboratory of Public Health, Department of Environmental Veterinary Sciences,
Graduate school of Veterinary Medicine, Hokkaido University, Sapporo, Japan

CONTENTS

[Chapter II]

Identification and analysis of host proteins interacting with the 3'-untranslated region of tick-borne encephalitis virus.

Abbreviations

BHK	baby hamster kidney
C	capsid
CPE	cytopathic effect
CSDE1	Cold shock domain-containing E1
DENV	Dengue virus
DMEM	Dulbecco's Modified Eagle's medium
DNA	deoxyribonucleic acid
E	envelope
EGFP	enhanced green fluorescence protein
FBS	fetal bovine serum
FMRP	fragile X mental retardation protein
HCV	Hepatitis C virus
HEK293T	human embryonic kidney 293T
IC	infectious clone
IFA	immunofluorescence assay
ILF2	interleukin enhancer-binding factor 2
ILF3	interleukin enhancer binding factor 3
IP	immunoprecipitation
IRES	internal ribosome entry site
ISRE	interferon stimulated response element
JEV	Japanese encephalitis virus
KD	knock down
LC-MS/MS	liquid chromatography-tandem mass spectrometry
LGTV	Langat virus
MOI	multiplicity of infection
MTase	methyltransferase
NF 45	nuclear factor 45
NF 90	nuclear factor 90
NS	non-structural protein
ORF	open reading frame
PBS	phosphate buffered saline
PCR	polymerase chain reaction
PFU	plaque forming unit
p.i.	post infection
PKR	protein kinase R
prM	precursor membrane
p.t.	post transfection
RdRp	RNA dependent RNA polymerase

RNA	ribonucleic acid
RT-PCR	reverse transcription polymerase chain reaction
STRBP	spermatid perinuclear RNA binding protein
shRNA	short hairpin RNA
siRNA	small interfering RNA
SL	stem loop
TBE	Tick-borne encephalitis
TBEV	Tick-borne encephalitis virus
UTR	untranslated region
WNV	West Nile virus

Preface

Tick-borne encephalitis (TBE) virus (TBEV), a member of the genus Flavivirus in the family *Flaviviridae*, is a major arbovirus that causes thousands of cases of severe neurological illness annually (1). Humans are accidental hosts, who become infected by a tick bite or by consumption of raw milk from infected domestic animals. TBE has been a huge public health problem in endemic areas of European and Asian countries (2-4). Mortality rates vary from about 0.5 to 30%, and neurological sequelae can occur in 30 to 60% of survivors (5-7). Although vaccines are currently available, TBE is a significant public health problem in endemic areas of the European and Asian countries (3, 4)

TBEV is a positive-stranded RNA virus with a genome of ~11 kb that encodes a long polyprotein in a single open reading frame (ORF), flanked by 5′- and 3′-untranslated regions (UTRs). The corresponding polyprotein is processed into structural proteins, i.e., capsid (C), pre-membrane (prM), envelope (E) protein, as well as non-structural proteins (NS) NS1, NS2A, NS2B, NS3, NS4A, NS4B, and NS5(8, 9). The C protein is associated with the genome RNA packaging and neuropathogenesis of TBEV (10, 11). The M protein is initially translated as a precursor protein known as prM(12), forms a heterodimer with the E protein, and functions to protect the E protein. It is known that the E protein is responsible for binding to cellular receptors, tissue tropism and virulence, as well as for the induction of virus-neutralizing antibodies (13-15). The non-structural proteins play roles in the genome replication and the processing of viral proteins. NS3 functions as a protease (16, 17) and helicase (18), and NS5 functions as a methyltransferase (19), RNA-dependent RNA polymerase and interferon antagonist (20). The 5′- and 3′-UTRs are believed to be associated with viral genome replication (21, 22).

Based on phylogenetic analysis, TBEV can be divided into three subtypes: the Far-Eastern, Siberian and European subtype (7). Each subtype causes different symptoms and mortality (3, 23). The Far-Eastern subtype is also known as Russian spring summer encephalitis virus, and is prevalent in Far-Eastern Russia. This subtype causes severe neural disorders such as encephalitis and meningoencephalitis with a high mortality rate up to 30 %(24). The Siberian subtype also causes less severe disease (case mortality rate, 7 to 8%) than the Far-Eastern subtype and is often associated with chronic disease (7). The European subtype produces biphasic febrile illness and milder encephalitis, and the mortality rate is lower than 2% (25).

The ranges of the Far-Eastern and the Siberian subtypes is expected to overlap in Mongolia between northern China and the Asian part of Russia (26, 27). Mongolia is also thought to be a TBE endemic region (28). Severe TBE cases have been reported since the 1980s in Selenge aimag and Bulgan aimag (near the border with Russia) (29). However, detailed information on the biological characteristics of the endemic viruses is still unclear. In this study, TBEV was isolated from the northern part of Mongolia. The biological characteristics such as viral multiplication and the pathogenicity were examined to evaluate the epidemiological risk of TBE in Mongolia [Chapter I].

The 3′-UTR of TBEV is divided into two domains: the 5′-terminal variable region and 3′-terminal core element. The core element is highly conserved among TBEV strains and contains a sequence that is essential for viral genome replication (21). The sequence and length of the variable region vary among TBEV strains. The variable region is previously considered that it’s not involved in the viral replication and virulence in

mice(30). A deletion or insertion of polyA sequence exists in the variable region of some strains (31). Strains isolated from ticks and wild rodents rarely contain a deletion or insertion of polyA sequence in the variable region, and this region is considered to be essential for the natural transmission cycle of TBEV (32). In contrast, deletions or insertion of polyA sequence in the variable region were found in strains passaged in mammalian cell culture or suckling mouse brain. Deletions were also observed in the TBEV strains isolated from human patients (30, 33, 34). These reports suggest that the deletion or the insertion of polyA sequence is caused by viral adaptation to mammalian cells and is related to the virulence causing severe case in human. However, the role of this region remains unclear.

The virus strain Sofjin-HO was isolated from a patient in Russia in 1937 and has been used as a prototype of the Far-Eastern subtype (35). It is also known to be highly pathogenic in a mouse model. The strain Oshima 5-10 was isolated from a sentinel dog in 1995 in the area in which a human case of TBE was reported in Japan, and was classified as the Far-Eastern subtype of TBEV. Oshima 5-10 is less virulent than Sofjin-HO in a mouse model (36). The nucleotide homology between Oshima 5-10 and Sofjin-HO is high (96%) with differences of only 44 amino acids and a deletion of 207 nucleotides exists in the 3’-UTR of Sofjin-HO. However, there is no information concerning the detailed mechanisms of different virulence in the two closely related strains.

Previous study showed that the 3'-UTR variable region is an important factor that determines the virulence of the Far-Eastern subtype of TBEV (37). It also suggested viral pathogenicity mediated by the 3’-UTR might be related to interaction with host factors *in vivo*. In this study, I tried to evaluate how the 3’-UTR and host factors were

involved in the pathogenicity of TBEV infection [Chapter II].

[Chapter I]

Isolation and characterization of Tick-borne encephalitis virus from *Ixodes persulcatus* in Mongolia in 2012.

Introduction

TBEV has been divided into three subtypes: the European subtype, the Siberian subtype and the Far-Eastern subtype (24). These subtypes cause different symptoms and mortality (7). The European subtype, which is distributed throughout Europe, causes a biphasic fever and milder form of encephalitis, and the mortality rate is up to 2% (25, 38). The distribution range of the Far-Eastern subtype covers Eastern Russia, northern China, and Japan. Infection with this subtype of TBEV provokes the most severe neural disorder, including encephalitis and meningoencephalitis, and the mortality rate is up to 30% (24). The Siberian subtype is widely distributed throughout Russia and the case mortality rate is 6 to 8%. Despite the milder form of encephalitis caused by Siberian subtype compared to the Far-Eastern subtype, humans infected with the Siberian subtype often develop chronic disease (7).

The ranges of the Far-Eastern and the Siberian subtypes is expected to overlap in Mongolia between northern China and the Asian part of Russia, respectively (26, 27). Mongolia is also a TBE endemic region (28). Severe TBE cases have been reported since the 1980s in Selenge aimag and Bulgan aimag (near the border with Russia) (29). In Bulgan aimag, the viral genome was detected in a patient in 2008 and from ticks in 2010 and these viral genes were clustered within the Far-Eastern subtype and the Siberian

subtype, respectively (29, 39). However, minimal data are available concerning the biological characteristics of Mongolian TBEV strains (e.g., virulence and viral multiplication).

In this study, ticks (*Ixodes persulcatus*) were collected from Selenge aimag in Mongolia, for the isolation of TBEV. I detected the TBEV antigens and genomic ribonucleic acid (RNA) in cell cultures inoculated with tick homogenates. Sequencing revealed that the isolated viruses belonged to the Siberian subtype of TBEV. Viral growth and plaque morphology were assessed and the pathogenicity of the viral isolates was analyzed in a mouse model.

Materials and Methods

Tick collection and virus isolation

TBEV strains were isolated from ticks (*I. persulcatus)* collected in Bugant village, Selenge aimag, in northern Mongolia, in 2012 (Fig. 1). In total, 680 ticks were collected by dragging flannel sheets over the vegetation and pooled into groups of 20-30 ticks. The pools were washed with ethanol and homogenized in phosphate buffered saline (PBS) with a pestle. Each homogenized suspension was centrifuged, and the supernatant was collected and stored at –80°C until the inoculation step.

Baby hamster kidney (BHK) cells were grown in 24-well plates. Then inoculated with the supernatants collected in the previous step, and incubated at 37°C under 5% CO_2 for 1 h. After 2 to 4 days, the cells were checked for cytopathic effect (CPE) and supernatants from cells showing a CPE were harvested and stored at –80°C. The viruses in these samples were identified by immunofluorescence assay (IFA) using anti-tick borne flavivirus antibodies and reverse transcription polymerase chain reaction (RT-PCR). All stock viruses were propagated once in BHK cells.

Detection of viral antigens

The tick homogenates were inoculated onto a monolayer of BHK cells. After 3 days of incubation at 37°C under 5% CO_2, the cells were fixed with 4% paraformaldehyde and permeabilized with 0.1% Triton X-100. After blocking with 2% bovine serum albumin, the cells were incubated with polyclonal hyper-immune murine ascites fluid from Langat virus (LGTV) infected mice (which is cross-reactive to TBEV), followed by Alexa 555-conjugated anti-mouse immunoglobulin G antibodies (Invitrogen, Carlsbad,

CA).

RT-PCR

Viral RNA was extracted from BHK cells using ISOGEN (Nippon Gene, Tokyo, Japan) and reverse-transcribed with random primers using M-MLV Reverse Transcriptase (Life Technologies, Carlsbad, CA). The TBEV-specific sequence was amplified with Platinum *Taq* polymerase (Invitrogen). To amplify the envelope (E) protein gene of TBEV, universal primers for the Far-Eastern and the Siberian subtypes of TBEV were designed and used. (Mongolia-F: 5'-GGT YAT GGA RGT YRC RTT CTC TCG-3', and Mongolia-R: 5'-TCC CAG GCG TGY TCT CCK ATC ACT GT-3').

TBE viral gene sequencing

The nucleic acid sequences of the viral genomes were determined by direct sequencing. The cycle sequencing reactions were performed using a BigDye Terminator Cycle Sequencing Kit (Life Technologies), and the sequences were determined with a 3130 Genetic Analyzer (Life Technologies). The primers used for sequencing were shown in Table 1.

Phylogenetic analysis

A phylogenetic analysis was performed using the complete E protein gene and the complete full sequence genomes of the TBEV strains. LGTV was used as the outgroup. Genetyx version 8 was used to generate the multiple alignments. MEGA 6 (http://www.megasoftware.net/) was used to generate phylogenetic trees by the neighbor-joining method. The reliability of the dendrogram was evaluated using 500 bootstrap

replicates. The GenBank Accession Numbers of the sequences were shown in Fig. 3.

Growth curve and plaque morphology assays in cell culture

For titration, BHK cell monolayers prepared in 12-well plates were incubated with serial dilutions of virus for 1 h, and then overlaid with minimal essential medium containing 2% fetal bovine serum (FBS) and 1.5% carboxymethyl cellulose and incubated for 4 days. The cells were then fixed and stained with crystal violet (0.25% in 10% buffered formalin) to visualize plaques. Plaques were counted and expressed as plaque-forming units (PFU).

Subconfluent BHK cells were grown in 12-well plates then inoculated with virus at a multiplicity of infection (MOI) of 0.01 PFU/ml. The cells were incubated at 37°C under 5% CO_2. Supernatants were harvested at 12, 24, 48, and 72 h post-infection (p.i.) and stored at –80°C until using for titration.

Cloning of full-length cDNA clone and recovery of virus.

The nucleotides 420–2295 of the prME protein gene were amplified from the MGL-Selenge-13-12 or MGL-Selenge-13-14 strain by RT-PCR and subcloned into the region of the full-length Oshima IC (the Far-Eastern subtype of TBEV) plasmid which has the SP6 promoter. Full-length bacterial clones were linearized with *Spe*I and transcribed into mRNA using the SP6-transcription system using mMESSAGE mMACHINE (Ambion). To recover virus, the mRNA was transfected to BHK cells. The full-length clone that produced infectious virus was designated as Oshima-MGL12-IC or Oshima-MGL14-IC. Recovered viruses were infected to BHK cells and viral antigen were detected by IFA using monoclonal antibodies to the E glycoprotein of TBEV or

polyclonal hyper-immune murine ascites fluid from LGTV infected mice.

Animal model

Each virus was inoculated subcutaneously at 10^3 PFU into ten 5-week-old female C57BL/6J mice (Japan SLC, Shizuoka, Japan). Surviving mice were monitored for 28 days p.i. to determine survival curves and mortality rates. Onsets of disease were estimated at 10% weight loss compared with the weight before virus infection. For the analysis of viral distribution in tissues, three to four mice were sacrificed on 3, 6, 9, 11 days p.i., and sera and brains were collected. Organs were individually weighted, homogenized, and prepared as 10% (w/v) suspensions in phosphate buffered saline with 10% fetal bovine serum. Suspensions were then clarified by centrifugation (5,000 rpm for 5min at 4°C), and the supernatants were titrated.

All animal experiments were performed in accordance with the Fundamental Guidelines for Proper Conduct of Animal Experiments and Related Activities in Academic Research Institutions under the jurisdiction of the Ministry of Education, Culture, Sports, Science and Technology. Experimental protocols were approved by the Animal Care and Use Committee of Hokkaido University (Approved No. V13025).

Results

Isolation and identification of TBEV in Mongolia

Nine strains of TBEV were isolated from *I. persulcatus* collected in Bugant village, Selenge aimag, Mongolia. BHK cells were inoculated with tick homogenates and the supernatants were blind passaged again. After incubation period for 2 to 4 days, CPE were observed in cells inoculated with nine homogenate pools. Viral-specific antigens and bands of viral sequence were detected in the cells by IFA and RT-PCR, respectively (Fig. 2). These isolates were identified as TBEV and designated as MGL-Selenge-13 strains (-5, -12, -13, -14, -15, -18, -19, -21, and -25).

Genetic analysis of the isolated TBEV strains

The nucleotide sequences of the viral E protein gene from the seven isolated MGL-Selenge-13 strains (-12, -13, -14, -15, -18, -19, and -21) and the complete genomic sequences of MGL-Selenge-13-12 and MGL-Selenge-13-14 were determined. A phylogenetic tree of the viral E protein gene and the open reading frame (ORF) is shown in Fig. 3. All isolated strains were classified as the Siberian subtype of TBEV and formed a similar cluster. The GenBank accession numbers of the viruses used in this study were shown in Fig. 3.

The nucleotide and amino acid sequence of the viral E protein gene were compared with MGL-Selenge-13-12, MGL-Selenge-13-14, MucAr M14/10 (isolated in Mongolia), 92M (isolated in Mongolia), and IR99 2f7 (isolated in Russia) (Table 2). All strains were highly homologous (>90%) in both their nucleotide and amino acid sequences. The full length sequences of MGL-Selenge-13-12 and MGL-Selenge-13-14

(11,106 nt) were also compared. The nucleotide homology was 99.1% (11005 nt /11106 nt) in the complete sequences, including the 5'- and 3'-untranslated regions (UTRs). Nucleotide substitutions were observed in the 5'-UTR (one nucleotide) and 3'-UTR (seven nucleotides), but no deletions or insertions were observed in these regions. The amino acid differences were located only in the viral E (residues 580, 597, and 631), NS3 (residues 1743, 1992, and 2046), and NS5 (residues 2623, 3221, 3223, 3352, 3357, 3403, and 3409) genes (Table 3).

Growth properties and pathogenicity of MGL-Selenge-13-12 and MGL-Selenge-13-14

The growth properties of MGL-Selenge-13-12 and MGL-Selenge-13-14 were compared with those of IR99 2f7 by monitoring viral release after infection. BHK cells were infected with each virus at an MOI of 0.01. Viruses were harvested at 12, 24, 48, and 72 h p.i., and the yields quantified using a plaque assay. The virus growth titers were similar among the MGL strains (Fig. 4A). MGL-Selenge-13-12 and MGL-Selenge-13-14 strains showed similar plaque size, while plaque size of IR99 2f7 was relatively large (Fig. 4B).

The pathogenicity of MGL-Selenge-13-12 and MGL-Selenge-13-14 was examined and compared with that of the other Siberian subtype strain, IR99 2f7, in a mouse model. Mice were infected subcutaneously with 10^3 PFU/mouse of each virus strain and survival rates were recorded over 28 days (Fig. 5). All mice infected with IR99 2f7 and MGL-Selenge-13-12 showed clinical symptoms such as a hunched posture, weight loss, ruffled fur, and general malaise. The mice with more severe disease showed neurological symptoms, including paralysis and loss of balance. The mice infected with

MGL-Selenge-13-14 showed significantly reduced symptoms compared to the mice infected with IR99 2f7 and MGL-Selenge-13-12 ($p<0.05$). The morbidity and mortality rates were significantly lower for mice infected with MGL-Selenge-13-14 than those for mice infected with IR99 2f7 or MGL-Selenge-13-12 (Fig. 5). The survival time and time to the onset of disease were longer for the MGL-Selenge-13-14 infected mice than for the IR99 2f7 or MGL-Selenge-13-12 infected mice (Table 4). These data indicate that MGL-Selenge-13-14 is less virulent than MGL-Selenge-13-12 in mice.

To examine the viral replication in organs, MGL-Selenge-13-12 and MGL-Selenge-13-14 strains were inoculated into mice. Viral multiplication in MGL-Selenge-13-12-infected mice sera were observed from 3 days p.i., but not in MGL-Selenge-13-14-infected mice sera (Fig. 6). The virus was detected in the brain from 9 days p.i. in all MGL-Selenge-13-12-infected mice and only one mice infected with MGL-Selenge-13-14 at 9 and 11 days p.i. respectively. The virus titer reached 8.9×10^7 PFU/ml at 11 days p.i. in the mice inoculated with MGL-Selenge-13-12 and was significantly higher than that in the mice infected with the MGL-Selenge-13-14 (Fig. 6).

Effect of the amino acid differences in the E protein

To examine the effect of the amino acid differences in the E protein between MGL-Selenge-13-12 and MGL-Selenge-13-14, the Oshima-MGL12-IC and Oshima-MGL14-IC viruses were constructed by the substitution of the E protein gene of the Oshima strain, Oshima-IC, with that of MGL-Selenge-13-12 and MGL-Selenge-13-14, respectively. All recombinant viruses produced virus antigen in the BHK cells at 4 days p.i (Fig. 7A). The supernatants were transferred to fresh BHK cell and Oshima-MGL12-IC and Oshima-IC produced distinct fluorescent foci of infected cells at 4 days p.i (Fig.

7B). However, Oshima-MGL14-IC showed few infected cells (Fig. 7B). These results indicate that amino acid differences within the E protein was responsible for the viral replication process.

Discussion

In this study, nine TBEVs (MGL-Selenge-13) were isolated from *I. persulcatus* collected in Bugant village, Selenge aimag, Mongolia (Figs. 1, and 2). The TBEV detection rate in ticks (1.3%) was similar to that in a previous study (1.6%) in Mongolia (29). TBEV infected human cases were found mainly in northern Mongolia, especially Selenge aimag (28). The Siberian subtype (92M and MucAr M14/10) of TBEV was also detected from a patient and ticks in northern Mongolia (29, 39). These results showed that the Siberian subtype of TBEV is endemic in northern Mongolia. This area is located next to the Asian part of Russia, which is known to be a severe TBEV endemic region (40). Human activity may have contributed to the transmission of TBEV from Siberian Russia to Mongolia via the Trans-Siberian railway (29, 41). Additionally, Mongolia is an important place for wild bird migration. There are transmission directions of influenza A virus between Russia and Mongolia via birds migration (42). Surveillance in Russia showed wild birds were bitten by ticks infected with TBEV (43). It is possible that wild birds may contribute to the transmission of TBEV into Mongolia.

From the phylogenetic analysis (Fig. 3A), the MGL-Selenge-13 strains were classified in the same subcluster as the Siberian subtype. Within the cluster of the Siberian subtype of Mongolian TBEV, the strains diverged into two subclusters. The MGL-Selenge-13 strains were classified in the same subcluster as the 92M strain but not the MucAr M14/10 strain. The MucAr M14/10 strain was in a subcluster with the IR99 2f7 strain isolated from Irkutsk (40). It has been reported that several subclusters of Siberian TBEV are endemic in Russia (44). My results suggest that at least two subclusters of TBEV invaded from Russia into Mongolia, independently.

The biological characteristics of the MGL-Selenge-13-12 and the MGL-Selenge-13-14 strains were compared (Fig. 4). The virus titer in BHK cells and the plaque size were almost same between the MGL-Selenge-13-12 and the MGL-Selenge-13-14 strains. However, the virulence of the MGL-Selenge-13-14 strain in mice was significantly lower than that of the MGL-Selenge-13-12 strain (Fig. 5). My results indicated the plaque morphology and size of the Mongolian isolates were not directly correlated with the neuroinvasiveness as shown in a previous study of TBEV isolates from Switzerland by Gaeumann et al (45). The death of mice infected with the MGL-Selenge-13-14 was delayed compared with that of mice infected with MGL-Selenge-13-12, and several mice recovered after the onset of disease. It was previously reported that a combination of central nervous system pathology and systemic inflammatory responses were involved in the late death of mice infected with some strains of TBEV (44). It is possible that these types of pathological features contributed to the difference in virulence between the MGL-Selenge-13-12 and the MGL-Selenge-13-14 strains.

Increased viral multiplication was observed in the blood and brain of the mice infected with MGL-Selenge-13-12 and it was significantly higher than those of MGL-Selenge-13-14-infected mice, although they showed similar growth properties in BHK cells (Figs. 4A and 6). These results indicated that the induction of the host immune responses might be different in the infection of the Mongolian isolates and that it affected the viral multiplication in the organs leading to the different virulence in the mice.

The complete genomic sequence of the MGL-Selenge-13-12 and the MGL-Selenge-13-14 strains differed by thirteen amino acids. Previous studies showed that naturally occurring mutations affect the pathogenicity of TBEV in nature (34, 46). In the viral E protein gene, it roles virus entry, three amino acids differences were located in

domains II and III. The analysis using chimeric infectious clones revealed that the amino acid differences in the E proteins between MGL-Selenge-13-12 and MGL-Selenge-13-14 affected the viral growth. It suggested that the differences in the E proteins might affect the virion entry or assembly step, resulting in the different virulence. In NS3, three amino acids differences were located in the C-terminal domain (residues 180-618), which possesses helicase activity (47). One amino acid difference was located in the N-terminal Methyltransferase (MTase) domain and six amino acids differences were in the C-terminal RNA-dependent RNA polymerase (RdRp) domain in NS5 (19, 48). Interestingly, the Cysteine residue at position 3,221 is strictly conserved within family *Flavivirdae* (48). It might be possible that the cysteine-to-tryptophan substitution in MGL-Selenge-13-14 strain affected the viral growth in mice (Table 2). Previous studies have shown that NS5 of flavivirus has an interferon antagonist activity which suppress innate immune responses (49, 50). To analyze the interferon antagonism of NS5 in MGL strains, reporter assays were performed for interferon stimulated response element (ISRE) promoter activity by interferon-β stimulation, but there was no significant difference between the MGL-Selenge-13-12 and the MGL-Selenge-13-14 strains (Data not shown). This result indicated that the interferon antagonism of NS5 were not associated with the different virulence between MGL-Selenge-13-12 and MGL-Selenge-13-14.

Several studies reported that the mutation of each of these proteins affected the virulence of TBEV (51-55). However, the different amino acids observed in the two Mongolian isolates have not been reported to be involved in the virulence in mice. Identification of the viral factor (mutation) responsible for the difference in virulence between the MGL-Selenge-13-12 and the MGL-Selenge-13-14 strains will lead to further

understanding of the functions of the viral protein in the pathogenicity of the Siberian subtype of TBEV.

In summary, I newly isolated the Siberian subtype of TBEV in Selenge aimag in Mongolia. Several strains showed different levels of virulence in a mouse model, indicating that a few naturally occurring mutations affect the virulence of the endemic strains in Mongolia. Minimal data are available about TBEV, which is endemic in Mongolia due to the lack of established diagnostic systems for TBE. Moreover, the Far-Eastern subtype of TBEV was also detected in other survey in Mongolia (39). To determine the distribution of TBEV in Mongolia, additional epidemiological studies are necessary. This results could be an important platform for monitoring TBEV to evaluate the epidemiological risk in TBE endemic areas of Mongolia.

Summary

Tick-borne encephalitis virus (TBEV) is a zoonotic virus belonging to the genus *Flavivirus,* in the family *Flaviviridae*. The virus, which is endemic in Europe and northern parts of Asia, causes severe encephalitis. Tick-borne encephalitis (TBE) has been reported in Mongolia since the 1980s, but details about the biological characteristics of the endemic virus are lacking. In this study, 680 ticks (*Ixodes persulcatus*) were collected in Selenge aimag, northern Mongolia, in 2012. Nine Mongolian TBEV strains were isolated from tick homogenates. A sequence analysis of the E protein gene revealed that all isolates belonged to the Siberian subtype of TBEV. Two strains showed similar growth properties in cultured cells, but their virulence in mice differed. Whole genome sequencing revealed only thirteen amino acid differences between these Mongolian TBEV strains. These results suggest that these naturally occurring amino acid mutations affected the pathogenicity of Mongolian TBEV. These results may be an important platform for monitoring TBEV to evaluate the epidemiological risk in TBE endemic areas of Mongolia.

Table 1. Primers for sequencing of the whole genome of the MGL-13 TBEV strain

Primer name	Primer sequence (5' to 3')	position
IR19f	agattttcttgcacgtgcat	1-20
IR319r	ctgtttcagaggaactgaat	342-323
IR392f	taggcttgcaaagacg	392-407
IR500f	aaggggatggcactactgtg	497-516
IR748f	tcagtgctgattccgtc	748-764
IR1327r	ccttcacgcaagtcacaatg	1327-1308
IR1406f	cacatacgggggactacgtt	1406-1425
IR1837r	ttacatggccgctttttagg	1837-1818
IR2372f	tgggcctgaatatgaggaac	2372-2391
Mongolia-F	ggttgccgttgtgtggttgac	885-905
Mongolia-R	ttccggatagtatgcgtagttg	2571-2550
IR2475f	cgtagacaccgagcgtatg	2475-2493
IR3281f	ccgagttgtaagggagaagtgt	3282-3303
IR3385r	tcaccttgccactctctgtg	3385-3366
IR3787r	gagcaggcccactctcagctcgaac	3792-3768
IR3677f	agagcttggtgcgatac	3677-3693
IR4016f	tgaccgtgcactatggactg	4016-4035
IR4562f	tatggacactatcagaa	4562-4578
IR4717f	ggagtcggatatggcttcaa	4717-4736
IR4938f	ccagcctggagaactgctctt	4938-4958
IR5005r	ctttggctaggtctatcggt	5005-4986
IR5119f	aaaagccgacccaacctac	5119-5137
IR5913r	tccggcttgatgtttgttcgcc	5912-5891
IR6276f	gacaagccgaaactggacat	6276-6295
IR6459f	gggcgcagcatcggagacgtgct	6457-6479
IR7449f	ttgtctgatggcggtagtca	7448-7467
IR7796f	taaggaagggggaaaccaac	7796-7815
IR7945r	gggaggccgcatagtagga	7945-7927
IR8346f	tgggaacatcgtgaactcag	8346-8365
IR8797r	ccgctctcatgatgaccttt	8797-8778
IR9344r	tcaccctccatgtaacgca	9347-9329
IR9546r	gtccccctccatcattcggat	9549-9529
IR10162f	cagaacaaggaaagggtcacag	10162-10141
ONR5	tgataaggccgaacatggtg	10887-10906
HO1	agcgggtgtttttccgag	11106-11087

Table 2. Comparison of viral E protein gene nucleotide sequences and amino acid sequences

Nucleotide \ Amino acid	MGL-Selenge-13-12	MGL-Selenge-13-14	MucAr M14/10	92M	IR99 2f7
MGL-Selenge-13-12		99.4% (493/496 aa)	99.2% (492/496 aa)	98.8% (490/496 aa)	99.0% (491/496 aa)
MGL-Selenge-13-14	98.4% (1464/1488 bp)		99.4%(493/496 aa)	99.0% (491/496 aa)	99.2% (492/496 aa)
MucAr M14/10	94.6% (1407/1488 bp)	93.9% (1397/1488 bp)		99.6% (494/496 aa)	99.8% (495/496 aa)
92M	96.2% (1431/1488 bp)	96.2% (1432/1488 bp)	94.6% (1407/1488 bp)		99.4% (493/496 aa)
IR99 2f7	94.2% (1401/1488 bp)	93.8% (1395/1488 bp)	97.0% (1439/1488 bp)	94.6% (1407/1488 bp)	

Table 3. Amino acid differences between MGL-Selenge-13-12 and MGL-Selenge-13-14

Amino acid Position	Gene	MGL-Selenge-13-12	MGL-Selenge-13-14
580	Envelope	Arg	Lys
597	Envelope	Asn	Thr
631	Envelope	Asp	Glu
1743	NS3	Ser	Gly
1992	NS3	Val	Leu
2046	NS3	Pro	Ser
2623	NS5	Ala	Thr
3221	NS5	Cys	Trp
3223	NS5	His	Arg
3352	NS5	Leu	Pro
3357	NS5	Ile	Met
3403	NS5	Leu	Ser
3409	NS5	Leu	Met

Table 4. Mortality and morbidity of the virus infected mice

strain	morbidity[a] (%)	mortality (%)	day of onset (days)	survival time (days)
IR99 2f7	10/10[b] (100)	10/10[c] (100)	9.4 ± 1.8	12.7 ± 2.9
MGL-Selenge-13-12	10/10 (100)	8/10 (80)	10.3 ± 1.5	13.8 ± 1.6
MGL-Selenge-13-14	5/10 (50)	4/10 (40)	14.0 ± 4.3	17.3 ± 4.6

[a]Morbidity of mice was estimated by >10% of weight loss.

[b]Number of sick mice / number of infected mice.

[c]Number of dead mice / number of infected mice.

Fig. 1

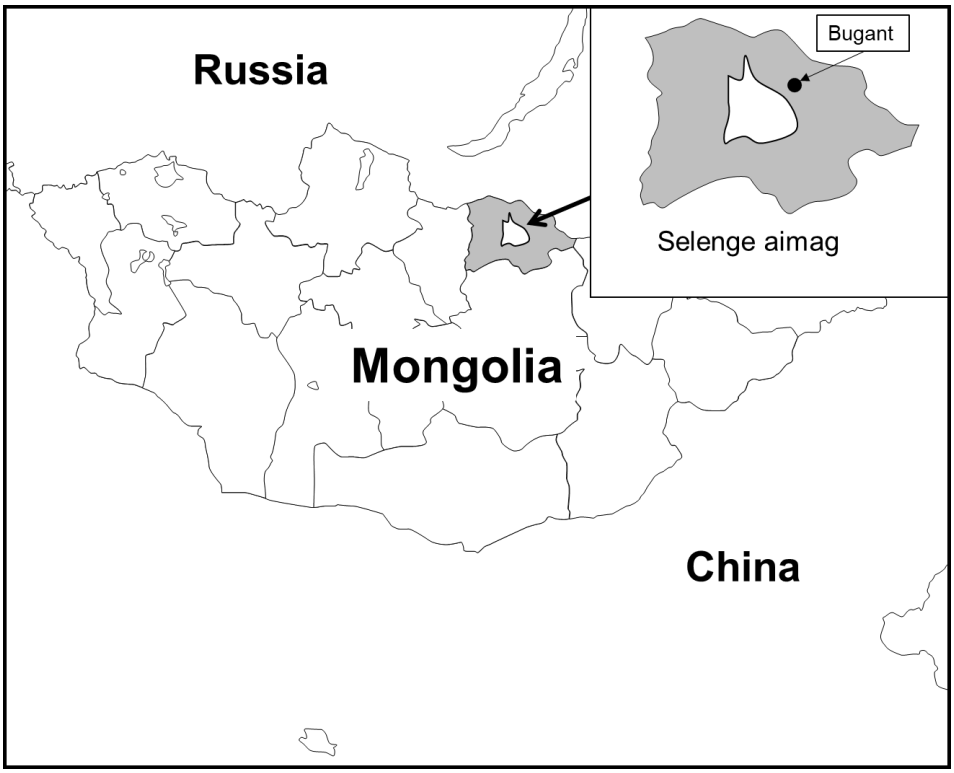

Fig. 1. Geographical distribution of the study area.

Fig. 2

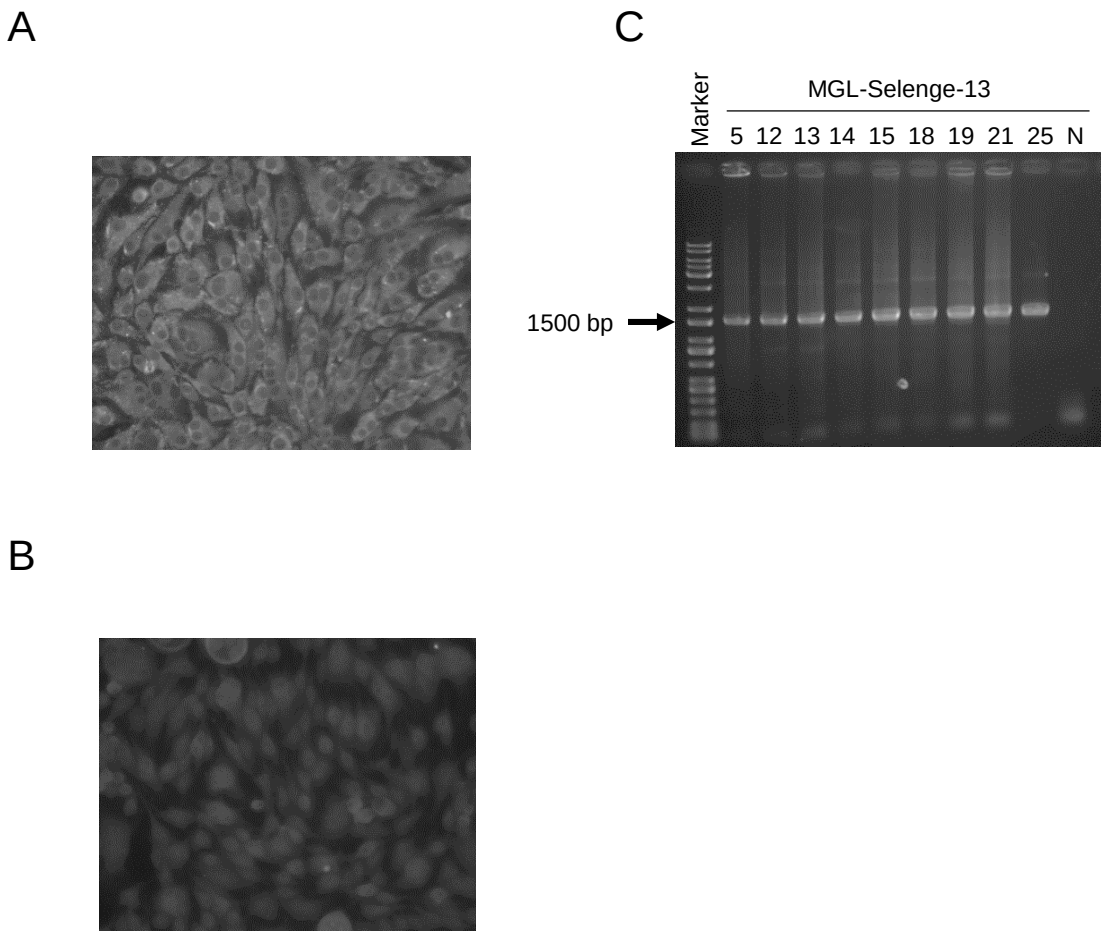

Fig. 2. Detection of TBEV specific antigens and RNA. (A and B) Immunofluorescence analysis of BHK cells. BHK cells were inoculated with the supernatant from tick homogenates. The TBEV antigen in the TBEV positive cells (MGL-Selenge-13-12) (A) or the negative cells (B) were detected with anti-tick borne flavivirus antibodies. (C) The E protein gene of TBEV (1488 bp) were amplified by RT-PCR from cells inoculated with TBEV positive tick homogenates (MGL-Selenge-13- 5, -12, -13, -14, -15, -18, -19, -21, and 25) and mock treated cells (N).

Fig. 3

A

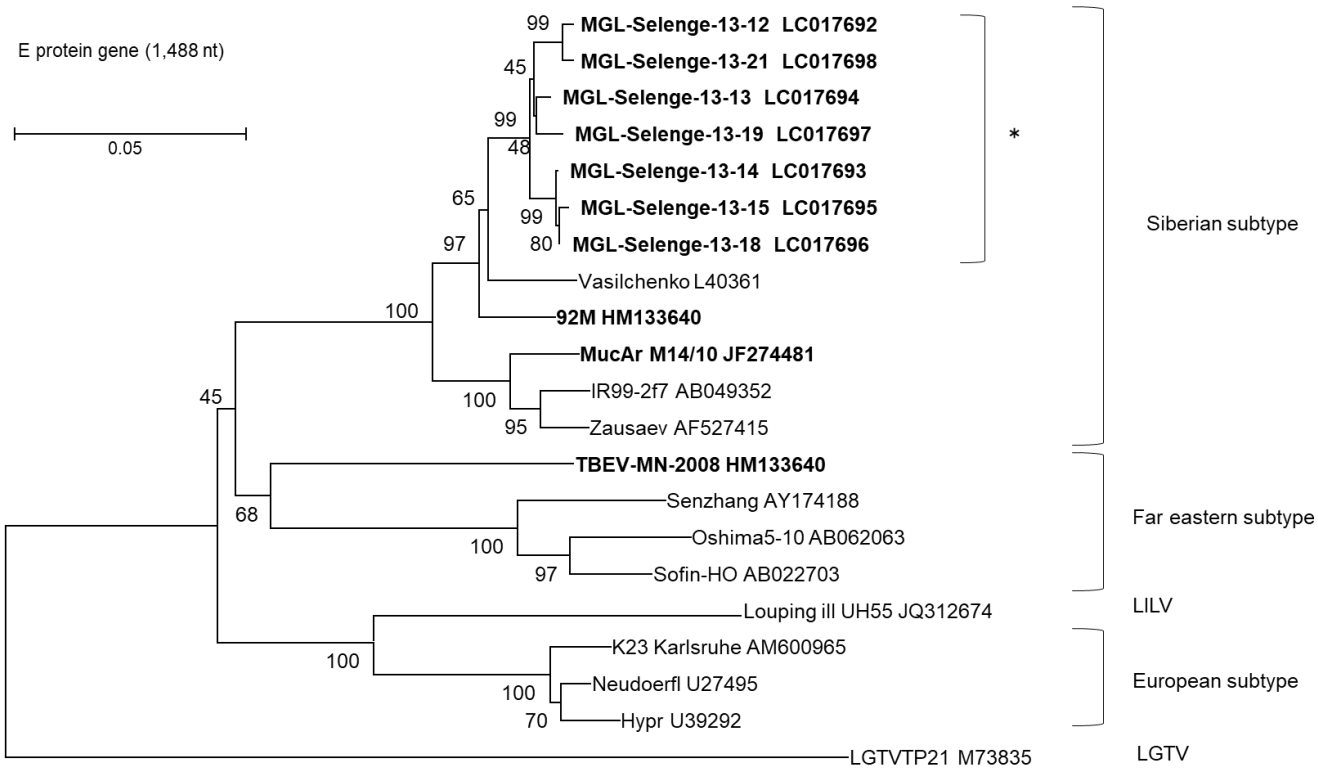

Fig. 3. (A) Phylogenetic tree of TBEV strains based on 1488 nucleotides of the viral E protein gene. LGTV was used as an outgroup. The percentage of bootstrap values are shown next to the branches. Asterisk indicated TBEV strains isolated in this study. Accession numbers are shown after the virus strains.

Fig. 3

B

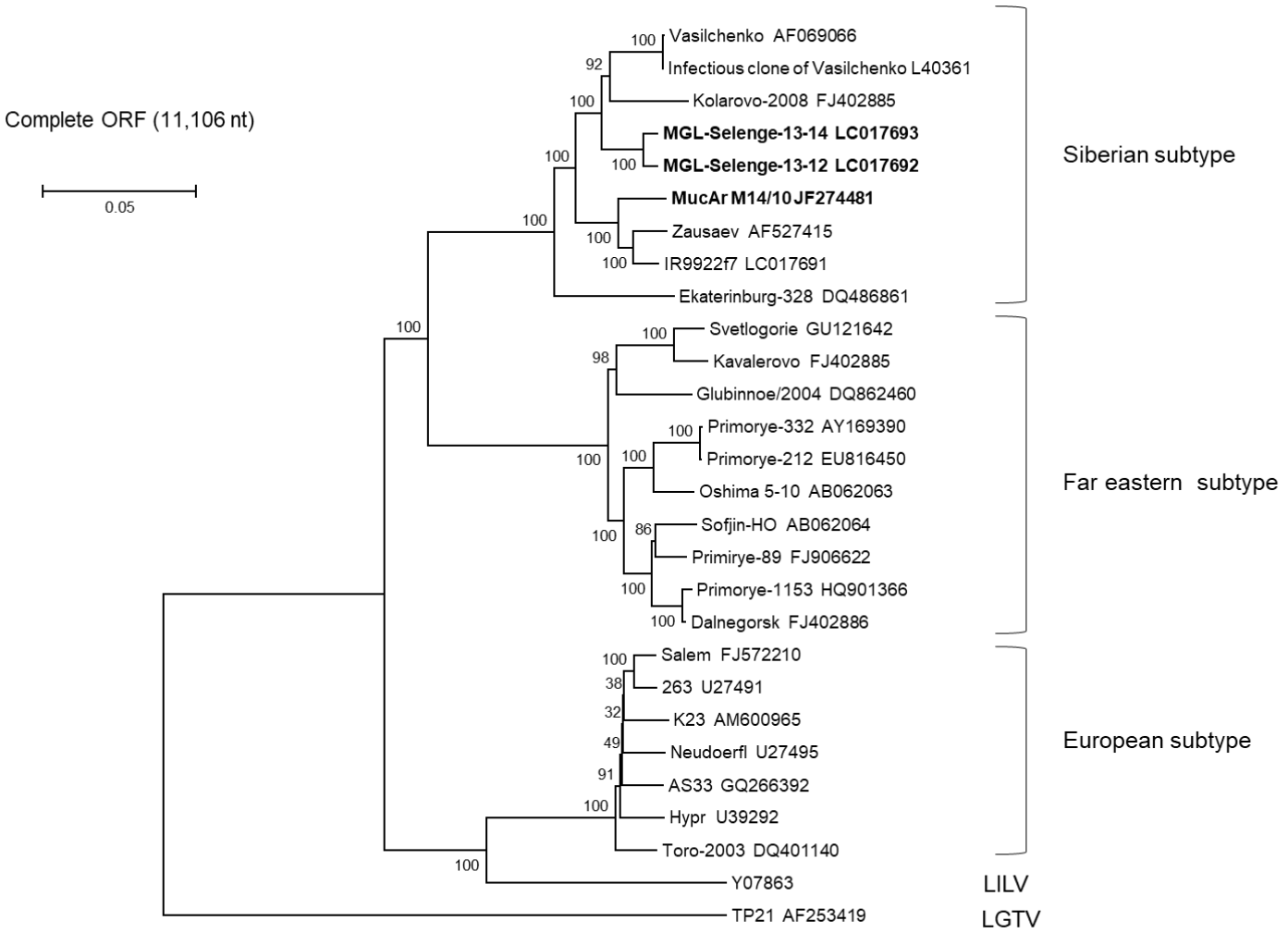

Fig. 3. (B) Phylogenetic tree of TBEV strains based on the ORF of the viral gene. LGTV was used as an outgroup. Bold letters indicate the strains isolated in Mongolia.

Fig. 4

A

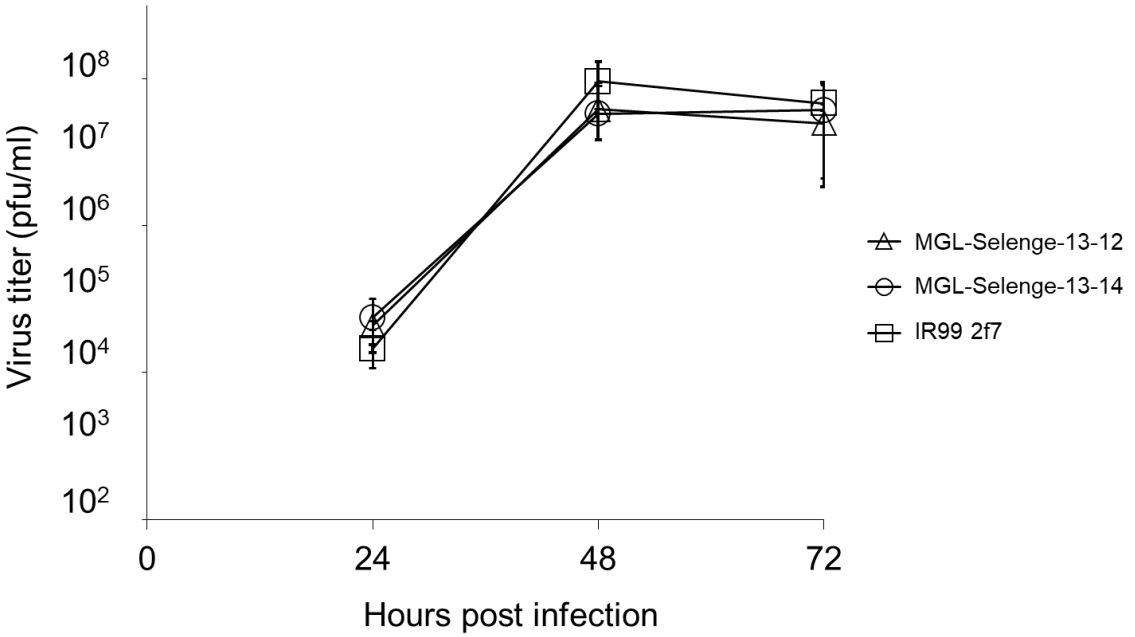

B

Fig. 4. (A) Comparison of the growth curves of IR99 2f7, MGL-Selenge-13-12, and MGL-Selenge-13-14. A monolayer of BHK cells was infected with each virus at a multiplicity of infection (MOI) of 0.01. At each time point, the medium was harvested and virus titers were determined using a plaque assay in BHK cells. (B) Plaque morphology of IR99 2f7, MGL-Selenge-13-12, and MGL-Selenge-13-14 in BHK cells. BHK cells were stained with crystal violet (0.1%) at 96 hours p.i.

Fig. 5

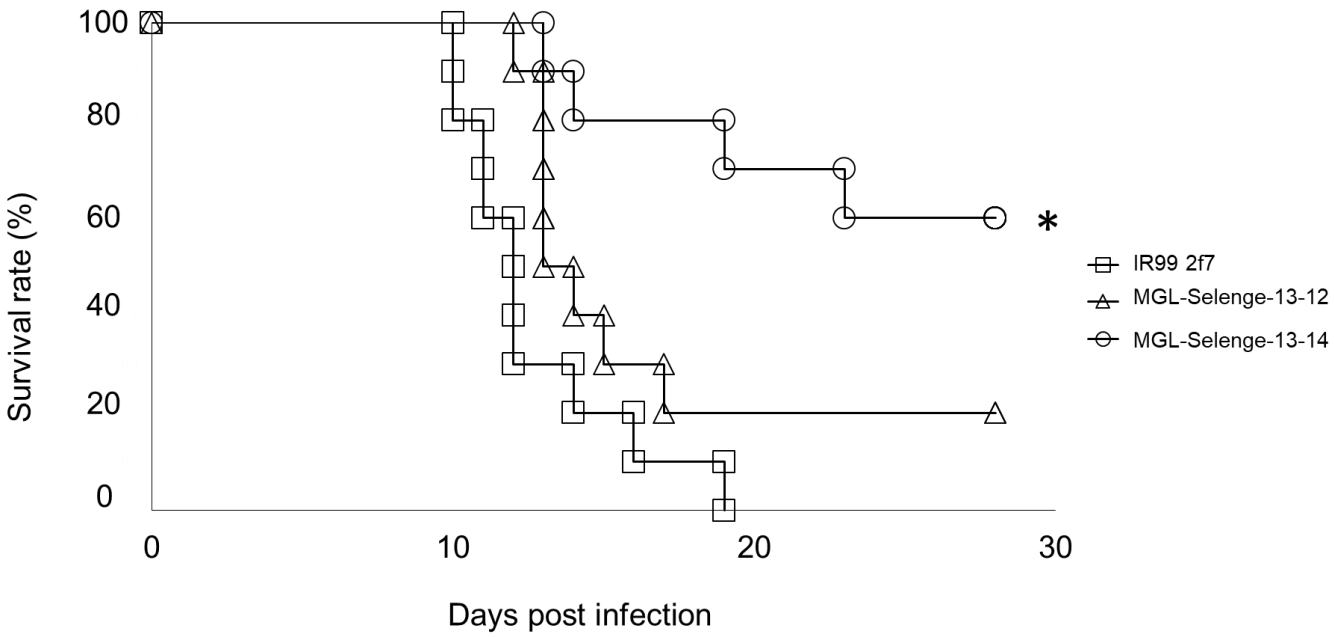

Fig. 5. Survival of mice inoculated with TBE viral strains IR99-2f7, MGL-Selenge-13-12, and MGL-Selenge-13-14. Mice were inoculated subcutaneously with 10^3 PFU of each virus and monitored for 28 days. Asterisk indicated significant differences in survival rate of MGL-Selenge-13-14 compared with IR99 2f7 and MGL-Selenge-13-12 ($p<0.05$). Survival rates were calculated using the Kaplan-Meier method and *p*-values for the differences in survival rates were calculated using log-rank tests.

Fig. 6

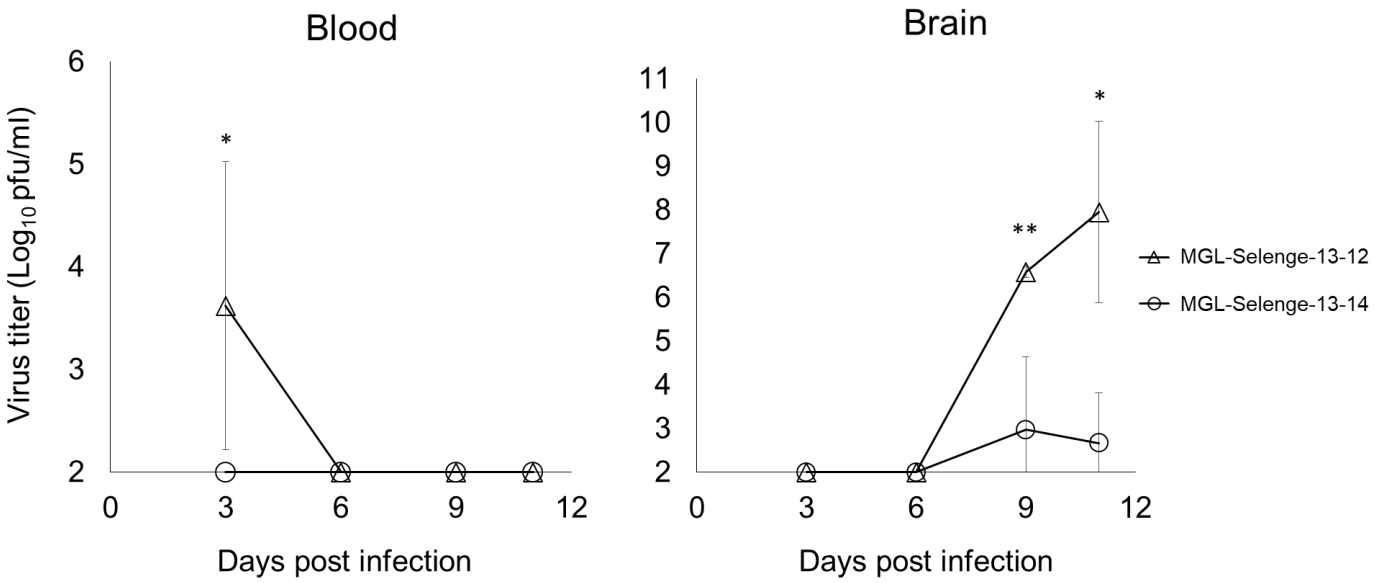

Fig. 6. Viral multiplication in mice organs. Mice were inoculated subcutaneously with 10^3 PFU of each virus. Virus titers in the blood and the brain at the indicated days after infection were determined by plaque assays. The limits of virus detection for the assay was 10^2 PFU/ml. Error bars represent the standard deviation (n=3 or 4). Asterisks indicate significant differences compared with MGL-Selenge-13-12 and MGL-Selenge-13-14 * (p<0.05) ** (p<0.01).

Fig. 7

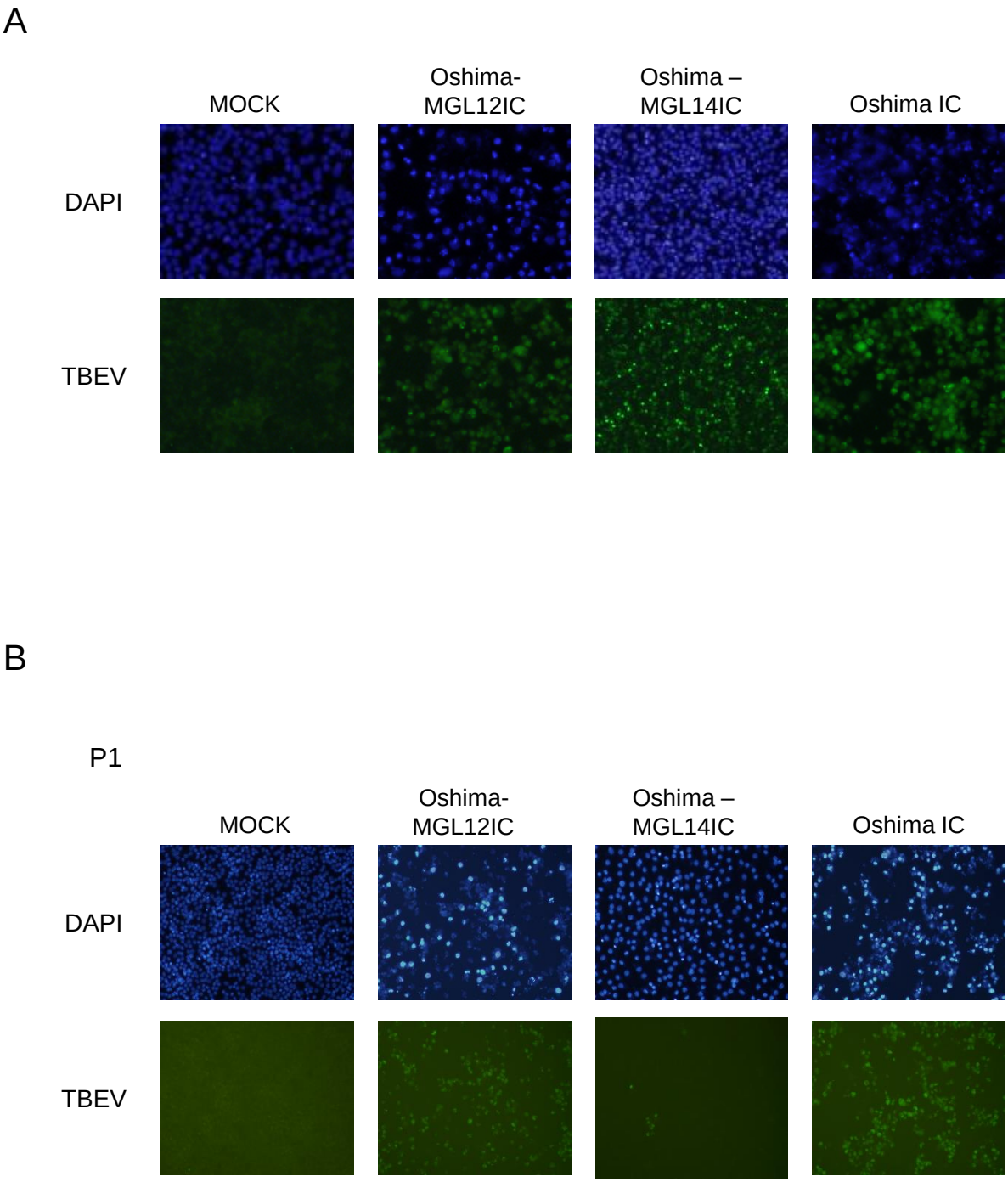

Fig. 7. (A) Immunostaining of cells transfected with Oshima-MGL12-IC, Oshima-MGL14-IC, Oshima-IC, or mock mRNA using specific anti-TBEV antibody at 4 days p.t. (B) Cells were inoculated with the supernatant viruses from the transfected cells, and viral antigen was stained with specific anti-TBEV antibody at 4 days p.i.

[Chapter II]

Identification and analysis of host proteins interacting with the 3’ -untranslated region of Tick-borne encephalitis viral genomic RNA.

Introduction

The variable region of the 3’-UTR is considered to be essential for the natural transmission cycle of TBEV, but it has been considered to play no role in viral replication and virulence in mammals (30). The sequence and length of the variable region vary among TBEV strains. Notably, strains isolated from ticks and wild rodents rarely contain deletions or polyA insertions in the variable region. In contrast, deletions or a polyA sequence insertion in the variable region were found in strains passaged in mammalian cell culture or isolated from human patients (33, 34, 56). Furthermore, a previous study revealed that partial deletions and polyA insertion in the variable region increased virulence in a mouse model (37, 57). These reports suggest that the deletions or polyA insertions are caused by viral adaptation to mammalian cells and are related to viral pathogenicity in severe cases in human. However, the role of this region in the virulence remains unclear.

Host factors binding to the viral 3’-UTR RNA has been shown to play important roles in mosquito-borne flavivirus, such as Dengue virus (DENV), Japanese encephalitis virus (JEV), and West Nile virus (WNV). The 3’-UTR of DENV was recognized by several components of stress granules, such as G3BP1, G3BP2 and Caprin, which

affected the antiviral responses through PKR-mediated innate immune response (58, 59). Several host proteins, such as La, p100, FBP1 and Mov34 were shown to bind to the 3′-UTRs of mosquito-borne flaviviruses affecting viral replication (60-64). However there is no report about the significance of the 3’-UTR in tick-borne flavivirus including TBEV.

In this study, I hypothesized that the difference in the variable region of the 3’-UTR of TBEV might affect the interaction with some host factors involved in the pathogenicity. Cellular proteins bound to the 3’-UTR RNA of TBEV were subjected to mass spectrometry (MS) analysis, and several proteins were identified to bind specifically to the low virulent Oshima strain. The mechanisms of the interaction was investigated and their role in viral replication was analyzed by RNA-silencing.

Materials and Methods

Cells and viruses

BHK cells were cultured in Eagle's minimum essential medium (Wako, Osaka, Japan) containing 8% FBS and penicillin/streptomycin (100 U/ml). Human embryonic kidney 293T (HEK293T) cells were cultured in high-glucose Dulbecco's Modified Eagle's medium (DMEM) (Wako) supplemented with 10% FBS and penicillin/streptomycin (100 U/ml). Human neuroblastoma SH-SY5Y cells were cultured in DMEM/Nutrient Mixture F-12 Ham (Sigma) supplemented with 10% FBS and penicillin/streptomycin (100 U/ml).

TBEV was prepared from infectious cDNA clones, Oshima-IC derived from the Oshima 5-10 strain (GenBank accession no. AB062063) (65), Oshima-Δ_SL3-5 with deletions of nucleotide 10,443–10,649, Oshima-Δ_SL3-4 with deletions of nucleotide 10,443–10,567, and Oshima-Δ_SL5 with deletions of nucleotide 10,568–10,649 (57), Sofjin-IC derived from the Sofjin-HO strain (GenBank accession no. AB062064) (66) as described previously. These viruses were stored at -80°C until use. Experiments using live TBEVs were conducted in Biosafety Level 3 or Animal Biosafety Level 3 facilities located at the Faculty of Veterinary Medicine at Hokkaido University.

Preparation of plasmid and RNA

Total RNA was extracted from HEK293T cells and subjected to reverse transcription PCR (RT-PCR) using gene specific primer sets (Table 5). To construct pCMV-Flag- Cold shock domain-containing E1 (CSDE1), fragile X mental retardation protein (FMRP), interleukin enhancer binding factor 3 (ILF3), PCR fragments of the

above gene were cloned into the pCMV-Flag plasmid.

For *in vitro* transcription of RNA, the 100 nucleotide of the 3' terminal of the coding sequence and the 3'-UTR of the Oshima or Sofjin strain, and the coding sequence for EGFP were cloned into pGEM-T Easy Vector. To prepare the RNA for the 3'-UTR of the Oshima strain with deletions, nucleotide for 10,443–10,649 (Δ_SL3-5), 10,443–10,567 (Δ_SL3-4), or 10,568–10,649 (Δ_SL5) was deleted by fused PCR, respectively. The plasmids were linearized by *Spe*I and RNA was transcribed using the MEGAscript T7 Kit (Life Technology) or Biotin RNA labeling kit (Roche) as following the instructions. The synthesized RNAs were stored at −80 °C until use.

RNA silencing and viral growth

For siRNA transfections, 1×10^5 SH-SY5Y cells were mixed with siRNA for CSDE1 (HSS111760 and HSS187882; Thermo) at a final concentration of 10 nM using Lipofectamine RNAiMax (Invitrogen) according to the manufacturer's protocol. At 24 hours post transfection (p.t.), the cells were inoculated with TBEV at a MOI of 0.05 PFU / cell and cultured for the indicated times. The supernatants were collected and stored at -80°C until use for viral titration.

Diluted culture supernatant from the infected cells was inoculated onto monolayers of BHK cells and incubated at 37°C for 1 h. The cells were overlaid with MEM containing 2% FBS and 1.5% methylcellulose and were incubated for 4 days. Plaques were visualized by staining with a 0.1% crystal violet solution in 10% formalin. A lentiviral vector that expresses a short hairpin RNA (shRNA) was generated by using pFU6-pGK puro vector. To knockdown (KD) the FMRP gene, oligonucleotides (shFMRP: 5'-CCGGGCGTTTGGAGAGATTACAAATCTCGAGATTTGTAATCTC-

TCCAAACGCTTTTTG-3'; was inserted into the *Eco*RI and *Bam*HI sites of the pFU6-pGK puro vector. HEK293T cells were transfected with the pFU6-pGK puro vectors and pLP1, pLP2, and pLP/VSVG plasmid using Polyethylenimine Max (Polysciences, Warrington, PA). Psuedotyped lentivirus were harvested from the supernatant at 48 h.p.t. SH-SY5Y cells were infected with lentivirus and selected with 6 μg/ml Puromycin for 1 week. Each cell was used for Western blotting and viral growth kinetics analysis.

Antibodies

The following antibodies were used for Western blot analysis and immunoprecipitation; rabbit polyclonal CSDE1 antibody (AB176584; Abcam): mouse monoclonal FMRP antibody (MAB2160; Merck): mouse monoclonal anti-Flag M2 antibodies (F3165: Sigma): mouse polyclonal ILF3 antibody (H00003609-B01P; Abnova): mouse monoclonal anti-beta actin (013-24553; Wako).

The immune complexes were detected by horseradish peroxidase-conjugated anti-mouse or rabbit antibodies and Immobilon Western HRP-Substrate (Merck).

Pull-Down assay of RNA binding Proteins

Streptavidin magnetic beads (GE Healthcare) were added to HEK293T cells lysed in RIPA buffer (50 mM Tris-HCl [pH 7.4], 150mM Nacl, 1% NP-40 substitute, 0.5% Sodium Deoxycholate, 0.1% Sodium DodecylSulphate, 1mM EDTA, 40U porcine RNase inhibitor, and 1× protease inhibitor cocktail), and incubated at 4°C for 1 h. Two hundred μg of protein from precleared HEK293T cell lysates were mixed with 1 μg of biotinylated RNA and Streptavidin magnetic beads (50% slurry) and further incubated at 4°C for 4 h. Beads were washed briefly three times with RIPA buffer and boiled in SDS

buffer, and the retrieved protein was analyzed by silver staining using 2D-Silver Stain Reagent II (Cosmo bio, Japan) and Western blotting. For the mass spectrometry analysis, co-precipitated beads were washed three times with cell lysis buffer and suspended in 2× SDS-PAGE sample buffer. The proteins were subjected to SDS-PAGE, followed by silver staining using SilverQuest staining kit (Invitrogen). The specific bands were cut from the gels, and each fraction was trypsinized and subjected to liquid chromatography-tandem mass spectrometry (LC-MS/MS) analysis to identify co-precipitated proteins. All of the proteins in gels were identified comprehensively, and the proteins detected in cells with the 3'-UTR RNA of TBEV but not in those with EGFP RNA were regarded as candidates for binding partners of the 3'-UTR of TBEV.

RNA immunoprecipitation

HEK293T cells were transfected with pCMV-Flag-based plasmid using X-tremeGENE HP DNA Transfection Reagent (Roche, Basel, Switzerland), following the manufacturer's instructions. At 48 h.p.t, the cells were washed with PBS and stored at -80°C. Cells were lysed in RIPA buffer, and cleared by centrifugation at 10,000 × *g* at 4°C for 10 min, and stored at −80°C until use. For immunoprecipitation, 1 mg of the total proteins were incubated with 1 μg of anti-Flag M2 antibody for 2 h at 4°C. Bound complexes were purified by 10 μl of SureBeads Protein G magnetic beads (Bio-Rad) with rotation at 4°C 1 h. After three times washing with RIPA buffer, immunoprecipitated proteins were analyzed by Western blotting. The RNA bound to Flag-tagged proteins were extracted from the beads with ISOGEN II (Nippon Gene). To detect TBEV RNA in the extracted RNAs, RT-PCR was conducted with SuperScript III (Thermo Fisher Scientific) and Platinum Taq DNA Polymerase (Thermo Fisher Scientific) with TBEV-specific

primers.

Mouse experiment

Total RNAs from the brain of the mice were extracted with ISOGEN II (Nippon Gene). Following RT-reaction with SuperScript III (Thermo Fisher Scientific), PCR was conducted using Platinum Taq DNA Polymerase (Thermo Fisher Scientific) with protein-specific primers. All procedures were performed according to the guidelines of the Animal Care and Use Committee of Hokkaido University (Approved No. V13025).

RESULTS

Identification of host proteins which bound to the 3'-UTR RNA of TBEV

To identify host proteins which bind to the 3'-UTR of TBEV, biotinylated RNAs for the 3'-UTR of the Oshima (Full) or Sofjin (Δ_SL3-5) strain or the coding sequence for EGFP as a control were mixed with HEK293T cell lysate and precipitated by Streptavidin beads (Fig. 8). The co-precipitated proteins were subjected to SDS-PAGE and stained by Silver staining (Fig. 9A). The RNA binding proteins specific to the viral RNA were detected around 72-90 kDa, and were subjected to MS analysis. The proteins showing the spectral and ion score over 200 were listed in Table 6. Keratin was excluded due to its high non-specificity in this test. Cold shock domain containing- E1 (CSDE1), interleukin enhancer binding factor 3 (ILF3), spermatid perinuclear RNA binding protein (STRBP), and fragile X mental retardation protein (FMRP), were identified as the RNA binding protein specific to the 3'-UTR of the Oshima strain. CSDE1, FMRP, and ILF3 were confirmed to be co-precipitated with the RNA for the 3'-UTR of the Oshima strain, but not for that of the Sofjin strain or the coding sequence for EGFP, by Western blot analysis using specific antibodies (Fig. 9B).

To further examine the specific interaction of the candidate proteins and viral 3'-UTR RNA, each protein with Flag-tag was overexpressed in HEK293T cells, and the cell lysate was mixed with *in vitro*-synthesized RNA and subjected to immunoprecipitation (IP) with anti-Flag antibody. Co-precipitated RNA was subjected to RT-PCR. The RNA for the full length 3'-UTR derived from the Oshima (Full) strain was co-precipitated with each RNA binding protein, but the RNA with the deletion observed in the Sofjin (Δ_SL3-5) strain was not (Fig. 10). These results indicated that several host proteins interacted to

the 3’-UTR RNA for the Oshima strain specifically, but not for the Sofjin strain.

Stem loop structures in variable region is essential for interaction with host proteins.

To investigate the viral RNA factor which differentiate the binding to the host proteins between Oshima and Sofjin strain, I conducted the pull down assay with *in vitro* synthesized RNAs. The variable region of the 3’-UTR of TBEV putatively forms seven stem loop (SL) structures. Oshima strain has all the seven SL (Full) structures, while the Sofjin strain has a deletion of the SL 3 to 5 (Δ_SL3-5) structures (nt 10443–10649).

To identify the region of the 3’-UTR of TBEV required for the binding to the host proteins, biotinylated Δ_SL3-4 or Δ_SL5 RNA were also prepared by introducing deletion of the SL 3 and 4 (nt 10,443–10,567), or the SL 5 (nt 10,568–10,649), respectively. And they were applied to pull down assay using streptavidin beads. Co-precipitated proteins were detected by immunoblotting (Fig. 11). All of three interacted with the Full, Δ_SL3-4, and Δ_SL5 RNA, but not with Δ_SL3-5 RNA (Fig. 11). These results indicated that the complete deletion from SL3 to SL5, but not the partial deletion among the SL3 to SL5 region, affected the interaction with each RNA binding protein.

Effect of the protein interacting with the 3’-UTR on virus replication

To examine the mRNA levels of CSDE1, FMRP, and ILF3 after viral infection, total RNA was extracted from brain inoculated with the Oshima-IC or Sofjin-IC and mRNA levels were compared with that of normal mice by RT-PCR using protein-specific primers. The mRNA levels of CSDE1, FMRP, and ILF3 were not affected by either Oshima-IC or Sofjin-IC infection (Fig. 12).

To investigate the role of CSDE1 and FMRP in viral replication, siRNA- or

shRNA-mediated gene silencing were performed in SH-SY5Y cells (Fig. 13). CSDE-KD cells showed no significant differences in the viral titers as compared to mock cells (Fig. 13A). In contrast, KD of FMRP reduced the viral titer of all virus strains (Fig. 13B). But, the viral titer of Oshima-IC was slightly recovered by the deletion of SL3-5 (Δ_SL3-5) ($p < 0.01$).

Discussion

In this study, host proteins binding to the 3'-UTR of TBEV were analyzed and 15 host factors were identified (Table 6). While three proteins were identified to bind to the 3'-UTR of the Oshima strain specifically, there were no host proteins interacting with only the 3'-UTR of the Sofjin strain. Most of the identified proteins were previously reported to be involved in mRNA metabolism, especially translation. In flavivirus study, PABPC1 was reported to be involved in circularization of the mRNA and enhancement of the translation efficiency and was shown to interact with the 3'-UTR of DENV (67). DDX21 was an established RNA helicase and negatively downregulated DENV replication (68). SYNCRIP was found to bind HCV RNA and enhance HCV internal ribosome entry site (IRES)-dependent translation and RNA replication (69, 70). Nucleolin also interacts and co-localizes with the DENV C protein and is required for production of infectious virus, suggesting the role in viral assembly (71). It is possible that these proteins may affect multiplication of viruses in the *Flaviviridae* in a common mechanism.

CSDE1, FMRP, and STRBP were shown to bind specifically to the 3'-UTR RNA of the low virulent Oshima strain, and higher MS score of ILF3 were observed in the host proteins co-precipitated with the 3'-UTR RNA of the Oshima strain than that of the highly virulent Sofjin strain. The Sofjin strain has complete deletion in the SL 3-5 structures, and these structures were shown to be recognized by host factors (Fig. 11). Deletion in the variable region in the 3'-UTR were found in strains passaged in mammalian cell culture or human patients (31, 34), suggesting that the deletion were the consequence of adaptation to mammalian species other than natural hosts. These indicated that the interaction of the host factors with the viral RNA via the SL structures

of the 3’-UTR might affect the attenuation of the pathogenicity of TBEV. One possible mechanism is that the deletion might arise through the escape from host anti-viral responses via the host factors recognizing the 3’-UTR. It was previously suggested that the variable region could act as a spacer separating the folded 3’-UTR structure from the rest of the genome that might be necessary for efficient binding of viral RNA polymerase and cellular factors involved in transcription. It is also possible that binding of the host proteins identified in this study may compete with that of the viral or host proteins involved in the efficient transcription.

CSDE1 is mostly localized in cytoplasm and is involved in the regulation of mRNA stability and translation (72). In recent study, CSDE1 was shown to bind the 3’-UTR of DENV and KD of CSDE1 reduced DENV replication (73), although no effect on TBEV replication was observed in this study (Fig. 13). The sequences and structures of the 3’-UTR were quite different between mosquito-borne and tick-borne flaviviruses, resulting in the different role of CSDE1 in replication of each flavivirus. It was also reported that CSDE1 was involved in the neural differentiation (74). Previous studies showed that TBEV infection affected neuronal functions, such as neurite development, in the neuro-pathogenicity (51, 75) , and it is possible that the interaction of CSDE1 might be involved in it.

ILF3 is known to have several transcript variants which forms a complex involved in neural transport (76). ILF3 and interleukin enhancer-binding factor 2 (ILF2) are also called nuclear factor 90 (NF90) and nuclear factor 45 (NF45), respectively, which form a protein complex involved in the post-transcriptional control of many genes in vertebrates (77). The ILF3/ILF2 complex is shown to be associated with the viral genomic RNA of HCV and DENV, through regulatory RNA structures in the 5′- and 3′-UTR within

viral replication foci in the cytoplasm (78, 79). STRBP is known as a paralogue of ILF3 and highly expressed in testis as well as in brain (80). ILF2 also recognizes STRBP and ZFR through the same binding interface with ILF3 (81). It was also reported that STRBP were involved in neuronal development in human and a mouse model (82, 83). It is possible the protein complex consisting of ILF3 paralogues and ILF2 might affect viral replication and neuropathogenicity.

FMRP is a protein that is highly expressed in neurons and is known as a part of a complex responsible for intracellular mRNA transport and also plays an important role in neuronal diseases in humans. In a previous study, FMRP was shown to bind the 5' UTR of TBEV genomic RNA, resulting in the development of neurological disease by TBEV infection (75). FMRP and ILF3 are involved in the formation of RNA granules (84, 85), which are large messenger ribonucleoprotein complexes controlling translation and mRNA translocation (86). Neuronal RNA granule also plays important roles in transport and local translation of mRNA in dendrites (87). In a previous study, RNA granules recognized viral RNAs inducing translation of interferon-stimulated mRNAs, and the antiviral responses were affected by RNAs derived from 3'-UTR of DENV (58). In this study, silencing of FMRP significantly reduced viral replication (Fig. 13B), indicating that the FMRP played important roles in TBEV replication. On the other hand, the deletion of the complete SL 3-5 structure increased the viral replication of Oshima-IC in FMRP-KD cells, and reduction of viral replication by FMRP-KD was relatively lower in Sofjin-IC infection. These results suggested that the deletion of the complete SL 3-5 structures compensated the TBEV replication without the binding of FMRP. However, the role of FMRP during viral infection *in vivo* could not investigate in this study. To determine the mechanisms of host-virus interaction, further analysis are required.

In summary, I identified host proteins binding to the 3’-UTR of TBEV genomic RNA. Some of them interacted with that of the low virulent strain specifically, and the SL structures in the 3’-UTR were involved in the interaction. Further analysis for the mechanism of interaction between the host proteins and viral RNA and the effect on viral infection will contribute to the understanding of pathogenicity of TBEV. It will also provide the information to design specific treatment of TBE targeting virus-host interaction.

Summary

Tick-borne encephalitis virus (TBEV) causes severe neurological disease in human, but the pathogenic mechanism is largely unclear. Previously, the conformational structure of the 3'-untranslated region (UTR) of TBEV was shown to be associated with the virulence. To clarify the host proteins which could interact with the 3'-UTR of TBEV, I tried to analyze the mechanisms of the interaction of the host proteins and the 3'-UTR of TBEV. Cellular proteins of HEK293T cells were co-precipitated with biotinylated RNAs of the 3'-UTR of low or highly virulent strain of TBEV, and were subjected to Mass spectrometry analysis. Fifteen host proteins were identified to bind to the 3'-UTR of TBEV, and four of them, CSDE1, STRBP, FMRP, and ILF3, bound that of the low virulent strain specifically. The RNA immunoprecipitation and pull down assay confirmed the interaction between the complete 3'-UTRs of TBEV genomic RNA and CSDE1, FMRP, or ILF3. The partial deletion of stem loop (SL) 3 to SL 5 structure of the variable region of the 3'-UTR did not affect the interaction with the host proteins, but the deletion of complete SL 3, 4, and 5 structures, which was observed in the highly virulent strain of TBEV, drastically reduce it. Further analysis of roles of the host proteins in the TBEV pathogenicity would lead to clarify the detailed mechanism of neurologic disease of TBEV.

Table 5. Primers for the construction of plasmid expressing each host protein

Primer name	**Primer sequence (5' to 3')**
CSDE1_Fw	TGACGATAAACTCGAATGGAGAACGTTTTTACTGTG
CSDE1_Rv	TGGATCCCCGCGGCCTTAGTCAATGACACCAGCTT
FMRP_Fw	TGACGATAAACTCGAATGGAGGAGCTGGTGGTG
FMRP_Rv	TGGATCCCCGCGGCCTTAGGGTACTCCATTCACG
ILF3_Fw	TGACGATAAACTCGAATGCGTCCAATGCGAATTTT
ILF3_Rv	TGGATCCCCGCGGCCTTATCTGTACTGGTAGTTCAT

Table 6. Identified proteins interactiong with the 3‘-UTR of TBEV by MS analysis

	Accession No.	Score*			Protein Description	Gene
		Oshima	Sofjin	EGFP		
1	CSDE1_HUMAN	1957		14	Cold shock domain-containing protein E1	CSDE1
2	ILF3_HUMAN	1922	958	261	Interleukin enhancer-binding factor 3	ILF3
3	NUCL_HUMAN	1547	1049	827	Nucleolin	NCL
4	STRBP_HUMAN	988			Spermatid perinuclear RNA-binding protein	STRBP
5	HNRPQ_HUMAN	733	611		Heterogeneous nuclear ribonucleoprotein Q	SYNCRIP
6	HNRPR_HUMAN	771	930		Heterogeneous nuclear ribonucleoprotein R	HNRNPR
7	FMR1_HUMAN	341			Fragile X mental retardation protein 1	FMR1
8	HS90B_HUMAN	589	650	313	Heat shock protein HSP 90-beta	HSP90AB1
9	DDX21_HUMAN	440	558	53	Nucleolar RNA helicase 2	DDX21
10	HS71A_HUMAN	373	187		Heat shock 70 kDa protein 1A	HSPA1A
11	HS90A_HUMAN	431	528	208	Heat shock protein HSP 90-alpha	HSP90AA1
12	HSP7C_HUMAN	434	192		Heat shock cognate 71 kDa protein	HSPA8
13	IF2B1_HUMAN	324	404	20	Insulin-like growth factor 2 mRNA-binding protein 1	IGF2BP1
14	PABP1_HUMAN	218	229		Polyadenylate-binding protein 1	PABPC1
15	ZFR_HUMAN	205	408		Zinc finger RNA-binding protein	ZFR

* Blank indicated the score under detection limit.

Fig. 8

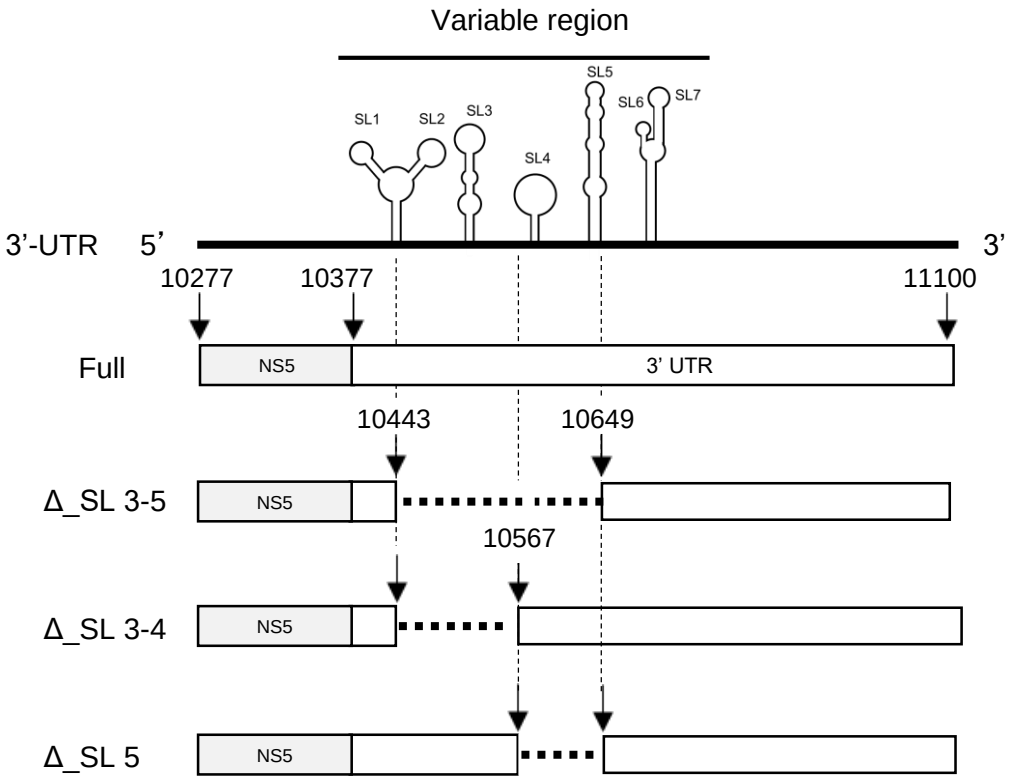

Fig. 8. Schematic of the 3'-UTR of TBEV genomic RNA.

Fig. 9

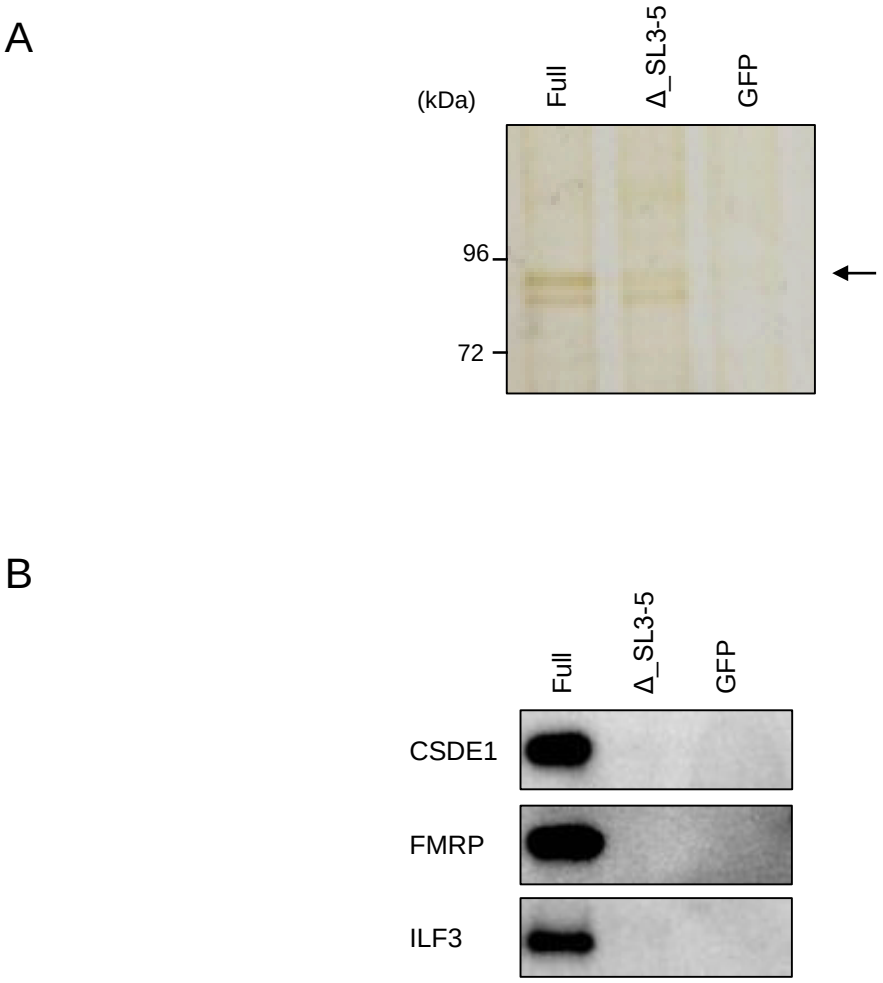

Fig. 9. Cellular proteins interacting with the 3'-UTR of TBEV. (A) The lysate from HEK293T cells were mixed with biotinylated RNA for the 3'-UTR of TBEV, and were precipitated with streptavidin beads. After SDS-PAGE, the proteins were stained by silver staining. The arrow indicated the bands for specific proteins which were subsequently subjected to MS analysis. (B) The co-precipitated proteins with the 3'-UTR of TBEV were analyzed by Western blotting. Each protein identified by MS analysis was detected by specific antibodies.

Fig. 10

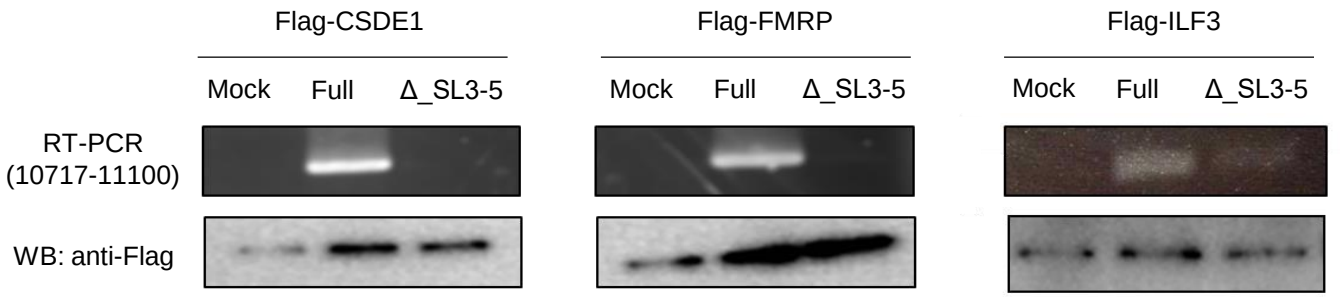

Fig. 10. Interaction of the host proteins with *in vitro*-synthesized RNA. The cell lysates overexpressing each Flag-tagged proteins were mixed with *in vitro*-synthesized RNA for the 3'-UTR of TBEV, and were precipitated by anti-Flag antibody. The RNA was extracted from immunocomplex and TBEV RNA was detected by RT-PCR. Upper panel shows Western blot analysis of immunoprecipitated protein by anti-Flag, and lower panel shows RT-PCR analysis of co-precipitated RNA.

Fig. 11

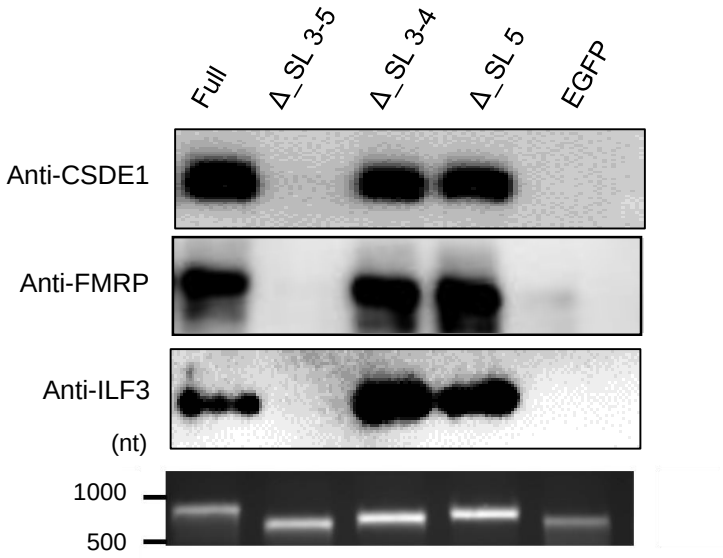

Fig. 11. Effect of deletions in the variable region on the interaction with the viral RNA and CSDE1, FMRP, or ILF3. Biotinylated RNA with or without deletion from SL3 to 5 structure of the 3'-UTR of TBEV were synthesized by *in vitro* transcription, and were incubated with HEK293T cell lysate and pulled down by streptavidin beads. The co-precipitated proteins were detected by anti-CSDE1, -FMRP, or -ILF3 antibody. The synthesized RNAs were applied to RT-PCR and detected by agarose gel electrophoresis.

Fig. 12

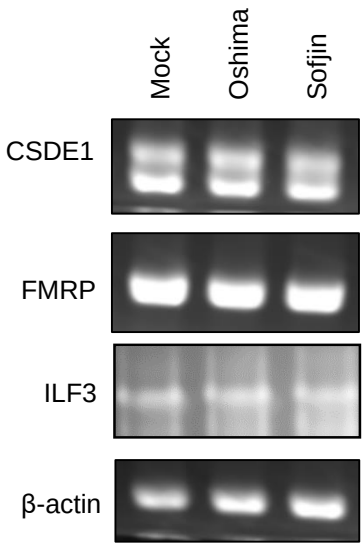

Fig. 12. Analysis of the mRNA levels in mice brain infected with TBEV. Total RNAs from the normal mice brain or the mouse brains infected with Oshima or Sofjin were subjected to RT-PCR using specific primers for each host factor. β-actin was used as loading control. Mock: normal mouse, Oshima: Oshima-infected mouse, Sofjin: Sofjin-infected mouse.

Fig. 13

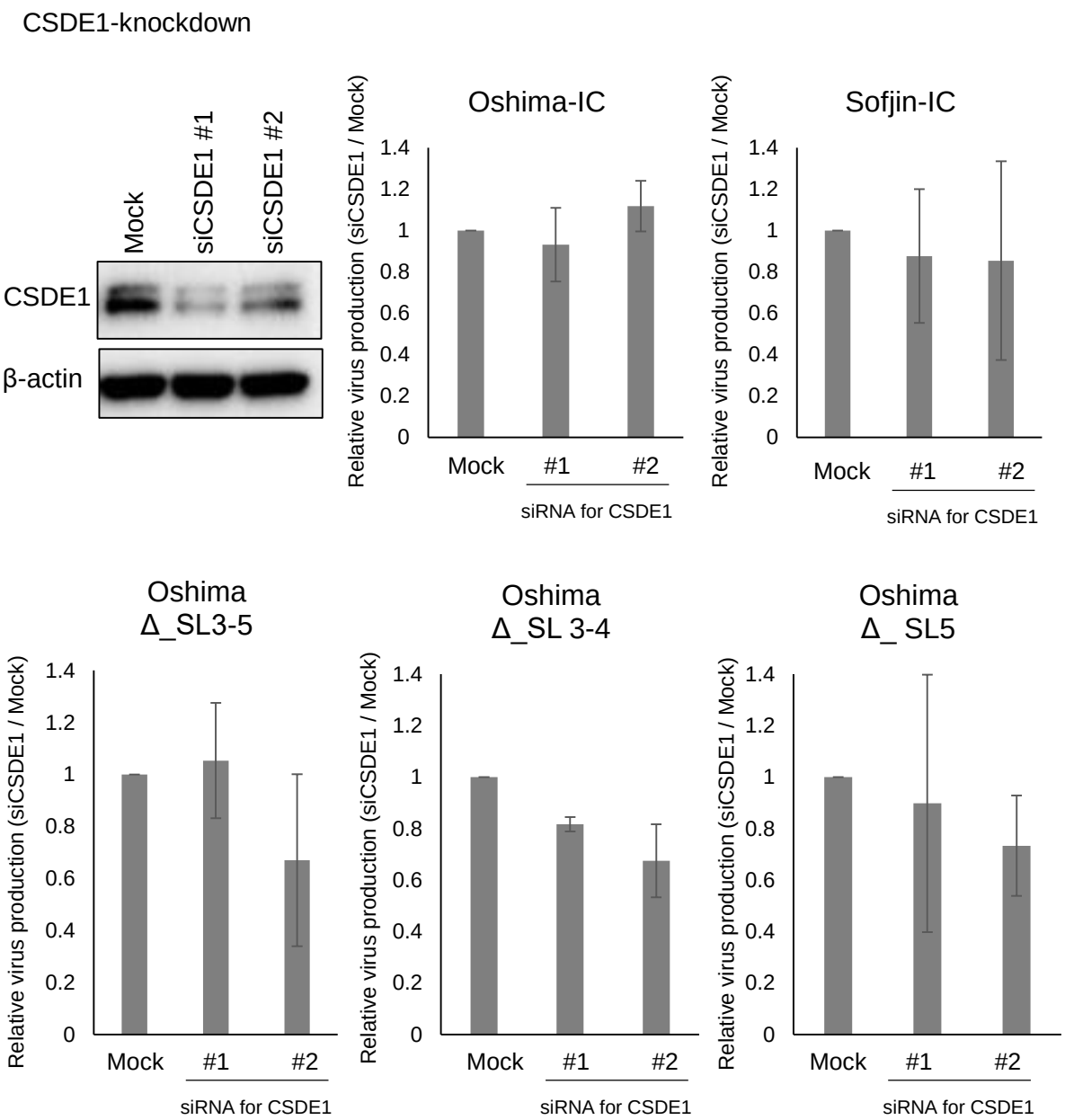

Fig. 13. Analysis of the the function of the host proteins in TBEV replication. (A) The effects of knockdown of CSDE1 on viral replication. CSDE1 was knocked down in SH-SY5Y cells by siRNA for CSDE1 (#1 and #2). The expression levels of CSDE1 in the cells transfected with each siRNA was analyzed by Western blotting. β-actin was used as loading control. CSDE1-KD cells were infected at an MOI of 0.05 with Oshima-IC, Sofjin-IC, Δ_SL3-4, Δ_SL5, or Δ_SL3-5, respectively. The supernatant from each cells was harvested at 18 h.p.i. and the viral titer was measured by plaque assay. Each viral titer was normalized as the ratio of viral titer in mock cells. Data represent mean ±S.D. of three independent experiments.

Fig. 13

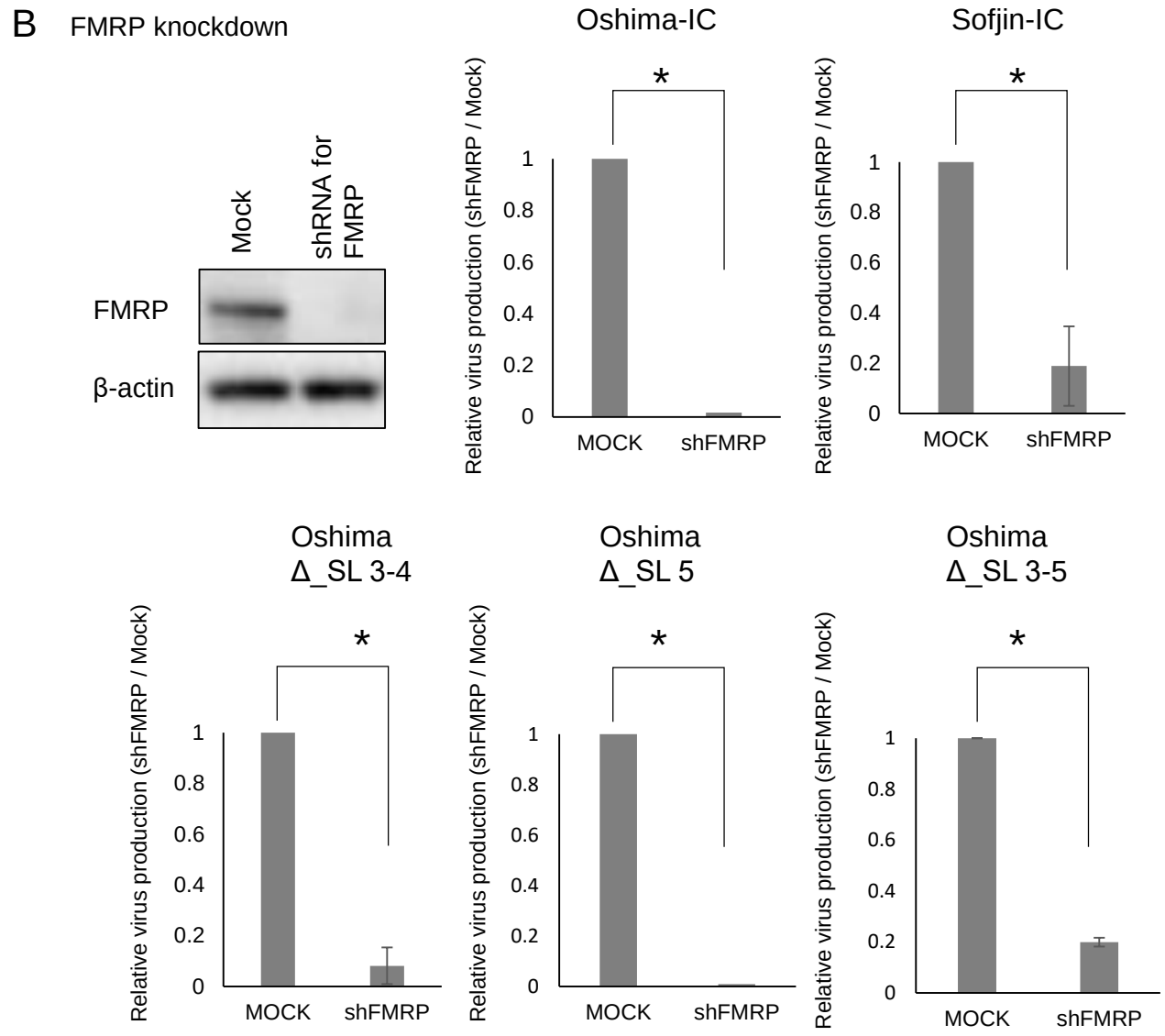

Fig. 13. (B) The effects of knockdown of FMRP on viral replication. FMRP was knocked down in SH-SY5Y cells by shRNA for FMRP. The expression levels of FMRP was analyzed by Western blotting. β-actin was used as loading control. FMRP-KD cells were infected at an MOI of 0.05 with Oshima-IC, Sofjin-IC, Δ_SL3-4, Δ_SL5, or Δ_SL3-5, respectively. The supernatant from each cells was harvested at 18 h.p.i. and the viral titer was measured by plaque assay. Each viral titer was normalized as the ratio of viral titer in mock cells. Data represent mean ±S.D. of three independent experiments. Statistical significance was assessed using the Steel test, and is indicated by asterisks (*, $p < 0.01$).

Conclusion

TBEV is a member of the genus Flavivirus in the family *Flaviviridae*, and is a major arbovirus that causes thousands of cases of severe neurological illness. Humans are accidental hosts, who become infected by a tick bite or by consumption of raw milk from infected domestic animals. TBE has been a huge public health problem in endemic areas of European and Asian countries.

Mongolia is also thought to be a TBE endemic region. Severe TBE cases have been reported since the 1980s in Selenge aimag and Bulgan aimag (near the border with Russia). However, detailed information on the biological characteristics of the endemic viruses is still unclear. In this study, I newly isolated the Siberian subtype of TBEV in Selenge aimag in Mongolia. Several strains showed different levels of virulence in a mouse model, indicating that a few naturally occurring mutations affect the virulence of the endemic strains in Mongolia. To determine the distribution of TBEV in Mongolia, additional epidemiological studies are necessary. My study could be an important platform for monitoring TBEV to evaluate the epidemiological risk in TBE endemic areas of Mongolia.

Next I tried to analyze the interaction between the host factor and viral RNA from low and high virulent TBE strains. The 3'-UTR variable region is an important factor that determines the virulence of the Far-Eastern subtype of TBEV. I identified host proteins binding to the 3'-UTR of TBEV genomic RNA. Some of them interacted with the 3'-UTR of the low virulent strain specifically, and the SL structures in the 3'-UTR were involved in the interaction. This study suggested that the whole conformational structure of the variable region is associated with the pathogenicity of the Far-Eastern

subtype of TBEV. My findings encourage further research to identify the pathogenic mechanisms of TBEV and develop prevention and therapeutic strategies for TBE.

Acknowledgements

I would like to extend my sincerest thanks and appreciation to my supervisors Professor Hiroaki Kariwa , Associate Professor Kentaro Yoshii, and Assistant professor Shintaro Kobayashi (Laboratory of Public Health, Faculty of Veterinary Medicine, Hokkaido University) for their mentorship and support.

Besides my advisor, I would like to thank the rest of my thesis committee: Professor Takashi Kimura (Laboratory of Comparative Pathology, Faculty of Veterinary Medicine, Hokkaido University) and Associate Professor Satoru Konnai (Laboratory of Infectious Diseases, Faculty of Veterinary Medicine, Hokkaido University) for their insightful comments and encouragement.

I would also like to thank the experts who were involved in the survey for Mongolian TBEV research project, Dr. Boldbaatar Bazartseren (Laboratory of Virology, Institute of Veterinary Medicine, Mongolian State University of Agriculture) [Chapter I]. I would also like to thank Associate professor Wataru Kamitani (International Research Center for Infectious Diseases, Research Institute for Microbial Diseases, Osaka University) who collaborate in the validation for Mass spectrometry analysis [Chapter II]

Finally, I wish to thank all the members of the laboratory of Public Health Faculty of Veterinary Medicine, Hokkaido University, for their support.

This work was supported by JSPS KAKENHI Grant Number 16J00854.

References

1. Who Publication. 2011. Vaccines against tick-borne encephalitis: WHO position paper--recommendations. Vaccine 29:8769-70.
2. Yoshii K, Song JY, Park SB, Yang J, Schmitt HJ. 2017. Tick-borne encephalitis in Japan, Republic of Korea and China. Emerg Microbes Infect 6:e82.
3. Lindquist L, Vapalahti O. 2008. Tick-borne encephalitis. Lancet 371:1861-1871.
4. Mansfield KL, Johnson N, Phipps LP, Stephenson JR, Fooks AR, Solomon T. 2009. Tick-borne encephalitis virus - a review of an emerging zoonosis. J Gen Virol 90:1781-94.
5. Heinz FX, Kunz C. 2004. Tick-borne encephalitis and the impact of vaccination. Arch Virol Suppl:201-5.
6. Grard G, Moureau G, Charrel RN, Lemasson JJ, Gonzalez JP, Gallian P, Gritsun TS, Holmes EC, Gould EA, de Lamballerie X. 2007. Genetic characterization of tick-borne flaviviruses: new insights into evolution, pathogenetic determinants and taxonomy. Virology 361:80-92.
7. Gritsun TS, Lashkevich VA, Gould EA. 2003. Tick-borne encephalitis. Antiviral Res 57:129-146.
8. Heinz FX, Allison SL. 2003. Flavivirus structure and membrane fusion. Adv Virus Res 59:63-97.
9. Chambers TJ, Hahn CS, Galler R, Rice CM. 1990. Flavivirus genome organization, expression, and replication. Annu Rev Microbiol 44:649-88.
10. Kofler RM, Leitner A, O'Riordain G, Heinz FX, Mandl CW. 2003. Spontaneous mutations restore the viability of tick-borne encephalitis virus mutants with large deletions in protein C. J Virol 77:443-51.
11. Kofler RM, Heinz FX, Mandl CW. 2002. Capsid protein C of tick-borne encephalitis virus tolerates large internal deletions and is a favorable target for attenuation of virulence. J Virol 76:3534-43.
12. Lobigs M. 1993. Flavivirus premembrane protein cleavage and spike heterodimer secretion require the function of the viral proteinase NS3. Proc Natl Acad Sci U S A 90:6218-22.
13. Navarro-Sanchez E, Altmeyer R, Amara A, Schwartz O, Fieschi F, Virelizier JL, Arenzana-Seisdedos F, Desprès P. 2003. Dendritic-cell-specific ICAM3-grabbing non-integrin is essential for the productive infection of human dendritic cells by mosquito-cell-derived dengue viruses. EMBO Rep 4:723-8.
14. Kopecký J, Grubhoffer L, Kovár V, Jindrák L, Vokurková D. 1999. A putative host cell receptor for tick-borne encephalitis virus identified by anti-idiotypic antibodies and

virus affinoblotting. Intervirology 42:9-16.

15. Kozlovskaya LI, Osolodkin DI, Shevtsova AS, Romanova LIu, Rogova YV, Dzhivanian TI, Lyapustin VN, Pivanova GP, Gmyl AP, Palyulin VA, Karganova GG. 2010. GAG-binding variants of tick-borne encephalitis virus. Virology 398:262-72.
16. Bazan JF, Fletterick RJ. 1989. Detection of a trypsin-like serine protease domain in flaviviruses and pestiviruses. Virology 171:637-9.
17. Fischl W, Elshuber S, Schrauf S, Mandl CW. 2008. Changing the protease specificity for activation of a flavivirus, tick-borne encephalitis virus. J Virol 82:8272-82.
18. Matusan AE, Pryor MJ, Davidson AD, Wright PJ. 2001. Mutagenesis of the Dengue virus type 2 NS3 protein within and outside helicase motifs: Effects on enzyme activity and virus replication. J Virol 75:9633-9643.
19. Egloff MP, Benarroch D, Selisko B, Romette JL, Canard B. 2002. An RNA cap (nucleoside-2 '-O-)-methyltransferase in the flavivirus RNA polymerase NS5: crystal structure and functional characterization. Embo J 21:2757-2768.
20. Park GS, Morris KL, Hallett RG, Bloom ME, Best SM. 2007. Identification of residues critical for the interferon antagonist function of Langat virus NS5 reveals a role for the RNA-dependent RNA polymerase domain. J Virol 81:6936-46.
21. Kofler RM, Hoenninger VM, Thurner C, Mandl CW. 2006. Functional analysis of the tick-borne encephalitis virus cyclization elements indicates major differences between mosquito-borne and tick-borne flaviviruses. J Virol 80:4099-113.
22. Khromykh AA, Meka H, Guyatt KJ, Westaway EG. 2001. Essential role of cyclization sequences in flavivirus RNA replication. J Virol 75:6719-28.
23. Gritsun TS, Frolova TV, Zhankov AI, Armesto M, Turner SL, Frolova MP, Pogodina VV, Lashkevich VA, Gould EA. 2003. Characterization of a siberian virus isolated from a patient with progressive chronic tick-borne encephalitis. J Virol 77:25-36.
24. Ecker M, Allison SL, Meixner T, Heinz FX. 1999. Sequence analysis and genetic classification of tick-borne encephalitis viruses from Europe and Asia. J Gen Virol 80 (Pt 1):179-85.
25. Dumpis U, Crook D, Oksi J. 1999. Tick-borne encephalitis. Clin Infect Dis 28:882-890.
26. Zhang Y, Si B-Y, Liu B-H, Chang G-H, Yang Y-H, Huo Q-B, Zheng Y-C, Zhu Q-Y. 2012. Complete genomic characterization of two tick-borne encephalitis viruses isolated from China. Virus Res 167:310-313.
27. Kulakova NV, Andaev EI, Belikov SI. 2012. Tick-borne encephalitis virus in Eastern Siberia: complete genome characteristics. Arch of Virol 157:2253-2255.
28. Walder G, Lkhamsuren E, Shagdar A, Bataa J, Batmunkh T, Orth D, Heinz FX,

Danichova GA, Khasnatinov MA, Wurzner R, Dierich MP. 2006. Serological evidence for tick-borne encephalitis, borreliosis, and human granulocytic anaplasmosis in Mongolia. Int J Med Microbiol 296:69-75.

29. Frey S, Mossbrugger I, Altantuul D, Battsetseg J, Davaadorj R, Tserennorov D, Buyanjargal T, Otgonbaatar D, Zoeller L, Speck S, Woelfel R, Dobler G, Essbauer S. 2012. Isolation, preliminary characterization, and full-genome analyses of tick-borne encephalitis virus from Mongolia. Virus Genes 45:413-425.
30. Mandl CW, Holzmann H, Meixner T, Rauscher S, Stadler PF, Allison SL, Heinz FX. 1998. Spontaneous and engineered deletions in the 3' noncoding region of tick-borne encephalitis virus: construction of highly attenuated mutants of a flavivirus. J Virol 72:2132-40.
31. Mandl CW, Kunz C, Heinz FX. 1991. Presence of poly(A) in a flavivirus: significant differences between the 3' noncoding regions of the genomic RNAs of tick-borne encephalitis virus strains. J Virol 65:4070-7.
32. Bredenbeek PJ, Kooi EA, Lindenbach B, Huijkman N, Rice CM, Spaan WJ. 2003. A stable full-length yellow fever virus cDNA clone and the role of conserved RNA elements in flavivirus replication. J Gen Virol 84:1261-8.
33. Leonova GN, Belikov SI, Kondratov IG, Takashima I. 2013. Comprehensive assessment of the genetics and virulence of tick-borne encephalitis virus strains isolated from patients with inapparent and clinical forms of the infection in the Russian Far East. Virology 443:89-98.
34. Formanova P, Cerny J, Bolfikova BC, Valdes JJ, Kozlova I, Dzhioev Y, Ruzek D. 2015. Full genome sequences and molecular characterization of tick-borne encephalitis virus strains isolated from human patients. Ticks Tick Borne Dis 6:38-46.
35. Barkhash AV, Perelygin AA, Babenko VN, Myasnikova NG, Pilipenko PI, Romaschenko AG, Voevoda MI, Brinton MA. 2010. Variability in the 2'-5'-oligoadenylate synthetase gene cluster is associated with human predisposition to tick-borne encephalitis virus-induced disease. J Infect Dis 202:1813-8.
36. Goto A, Hayasaka D, Yoshii K, Mizutani T, Kariwa H, Takashima I. 2002. Genetic and biological comparison of tick-borne encephalitis viruses from Hokkaido and far-eastern Russia. Jpn J Vet Res 49:297-307.
37. Sakai M, Muto M, Hirano M, Kariwa H, Yoshii K. 2015. Virulence of tick-borne encephalitis virus is associated with intact conformational viral RNA structures in the variable region of the 3'-UTR. Virus Res 203:36-40.
38. Suss J. 2008. Tick-borne encephalitis in Europe and beyond--the epidemiological situation as of 2007. Euro Surveill 13.

39. Khasnatinov MA, Danchinova GA, Kulakova NV, Tungalag K, Arbatskaia EV, Mironova LV, Tserennorov D, Bolormaa G, Otgonbaatar D, Zlobin VI. 2010. [Genetic characteristics of the causative agent of tick-borne encephalitis in Mongolia]. Vopr Virusol 55:27-32.
40. Hayasaka D, Ivanov L, Leonova GN, Goto A, Yoshii K, Mizutani T, Kariwa H, Takashima I. 2001. Distribution and characterization of tick-borne encephalitis viruses from Siberia and far-eastern Asia. J Gen Virol 82:1319-1328.
41. Kovalev SY, Chernykh DN, Kokorev VS, Snitkovskaya TE, Romanenko VV. 2009. Origin and distribution of tick-borne encephalitis virus strains of the Siberian subtype in the Middle Urals, the north-west of Russia and the Baltic countries. J Gen Virol 90:2884-92.
42. Kang H-M, Batchuluun D, Kim M-C, Choi J-G, Erdene-Ochir T-O, Paek M-R, Sugir T, Sodnomdarjaa R, Kwon J-H, Lee Y-J. 2011. Genetic analyses of H5N1 avian influenza virus in Mongolia, 2009 and its relationship with those of eastern Asia. Vet Microbiol 147:170-175.
43. Mikryukova TP, Moskvitina NS, Kononova YV, Korobitsyn IG, Kartashov MY, Tyuten'kov OY, Protopopova EV, Romanenko VN, Chausov EV, Gashkov SI, Konovalova SN, Moskvitin SS, Tupota NL, Sementsova AO, Ternovoi VA, Loktev VB. 2014. Surveillance of tick-borne encephalitis virus in wild birds and ticks in Tomsk city and its suburbs (Western Siberia). Ticks Tick Borne Dis 5:145-151.
44. Hayasaka D, Nagata N, Fujii Y, Hasegawa H, Sata T, Suzuki R, Gould EA, Takashima I, Koike S. 2009. Mortality following peripheral infection with Tick-borne encephalitis virus results from a combination of central nervous system pathology, systemic inflammatory and stress responses. Virology 390:139-150.
45. Gaeumann R, Ruzek D, Muehlemann K, Strasser M, Beuret CM. 2011. Phylogenetic and Virulence Analysis of Tick-Borne Encephalitis Virus Field Isolates From Switzerland. J Med Virol 83:853-863.
46. Kentaro Y, Yamazaki S, Mottate K, Nagata N, Seto T, Sanada T, Sakai M, Kariwa H, Takashima I. 2013. Genetic and biological characterization of tick-borne encephalitis virus isolated from wild rodents in southern Hokkaido, Japan in 2008. Vector Borne Zoonotic Dis 13:406-14.
47. Lescar J, Luo DH, Xu T, Sampath A, Lim SP, Canard B, Vasudevan SG. 2008. Towards the design of antiviral inhibitors against flaviviruses: The case for the multifunctional NS3 protein from Dengue virus as a target. Antiviral Res 80:94-101.
48. Selisko B, Dutartre H, Guillemot J-C, Debarnot C, Benarroch D, Khromykh A, Despres P, Egloff M-P, Canard B. 2006. Comparative mechanistic studies of de novo

RNA synthesis by flavivirus RNA-dependent RNA polymerases. Virology 351:145-158.

49. Best SM, Morris KL, Shannon JG, Robertson SJ, Mitzel DN, Park GS, Boer E, Wolfinbarger JB, Bloom ME. 2005. Inhibition of interferon-stimulated JAK-STAT signaling by a tick-borne flavivirus and identification of NS5 as an interferon antagonist. J Virol 79:12828-12839.

50. Lin RJ, Chang BL, Yu HP, Liao CL, Lin YL. 2006. Blocking of interferon-induced Jak-Stat signaling by Japanese encephalitis virus NS5 through a protein tyrosine phosphatase-mediated mechanism. J Virol 80:5908-18.

51. Yoshii K, Sunden Y, Yokozawa K, Igarashi M, Kariwa H, Holbrook MR, Takashima I. 2014. A Critical Determinant of Neurological Disease Associated with Highly Pathogenic Tick-Borne Flavivirus in Mice. J Virol 88:5406-5420.

52. Mandl CW, Allison SL, Holzmann H, Meixner T, Heinz FX. 2000. Attenuation of tick-borne encephalitis virus by structure-based site-specific mutagenesis of a putative flavivirus receptor binding site. J Virol 74:9601-9609.

53. Belikov SI, Kondratov IG, Potapova UV, Leonova GN. 2014. The Relationship between the Structure of the Tick-Borne Encephalitis Virus Strains and Their Pathogenic Properties. Plos One 9.

54. Goto A, Hayasaka D, Yoshii K, Mizutani T, Kariwa H, Takashima I. 2003. A BHK-21 cell culture-adapted tick-borne encephalitis virus mutant is attenuated for neuroinvasiveness. Vaccine 21:4043-4051.

55. Rumyantsev AA, Murphy BR, Pletnev AG. 2006. A tick-borne Langat virus mutant that is temperature sensitive and host range restricted in neuroblastoma cells and lacks neuroinvasiveness for immunodeficient mice. J Virol 80:1427-1439.

56. Mandl CW, Aberle JH, Aberle SW, Holzmann H, Allison SL, Heinz FX. 1998. In vitro-synthesized infectious RNA as an attenuated live vaccine in a flavivirus model. Nat Med 4:1438-40.

57. Sakai M, Yoshii K, Sunden Y, Yokozawa K, Hirano M, Kariwa H. 2014. Variable region of the 3' UTR is a critical virulence factor in the Far-Eastern subtype of tick-borne encephalitis virus in a mouse model. J Gen Virol 95:823-35.

58. Bidet K, Dadlani D, Garcia-Blanco MA. 2014. G3BP1, G3BP2 and CAPRIN1 are required for translation of interferon stimulated mRNAs and are targeted by a dengue virus non-coding RNA. PLoS Pathog 10:e1004242.

59. Reineke LC, Kedersha N, Langereis MA, van Kuppeveld FJ, Lloyd RE. 2015. Stress granules regulate double-stranded RNA-dependent protein kinase activation through a complex containing G3BP1 and Caprin1. MBio 6:e02486.

60. De Nova-Ocampo M, Villegas-Sepúlveda N, del Angel RM. 2002. Translation

elongation factor-1alpha, La, and PTB interact with the 3' untranslated region of dengue 4 virus RNA. Virology 295:337-47.

61. Lei Y, Huang Y, Zhang H, Yu L, Zhang M, Dayton A. 2011. Functional interaction between cellular p100 and the dengue virus 3' UTR. J Gen Virol 92:796-806.

62. Chien HL, Liao CL, Lin YL. 2011. FUSE binding protein 1 interacts with untranslated regions of Japanese encephalitis virus RNA and negatively regulates viral replication. J Virol 85:4698-706.

63. Ta M, Vrati S. 2000. Mov34 protein from mouse brain interacts with the 3' noncoding region of Japanese encephalitis virus. J Virol 74:5108-15.

64. Vashist S, Anantpadma M, Sharma H, Vrati S. 2009. La protein binds the predicted loop structures in the 3' non-coding region of Japanese encephalitis virus genome: role in virus replication. J Gen Virol 90:1343-52.

65. Hayasaka D, Gritsun TS, Yoshii K, Ueki T, Goto A, Mizutani T, Kariwa H, Iwasaki T, Gould EA, Takashima I. 2004. Amino acid changes responsible for attenuation of virus neurovirulence in an infectious cDNA clone of the Oshima strain of tick-borne encephalitis virus. J Gen Virol 85:1007-18.

66. Takano A, Yoshii K, Omori-Urabe Y, Yokozawa K, Kariwa H, Takashima I. 2011. Construction of a replicon and an infectious cDNA clone of the Sofjin strain of the Far-Eastern subtype of tick-borne encephalitis virus. Arch Virol 156:1931-41.

67. Polacek C, Friebe P, Harris E. 2009. Poly(A)-binding protein binds to the non-polyadenylated 3' untranslated region of dengue virus and modulates translation efficiency. J Gen Virol 90:687-92.

68. Dong Y, Ye W, Yang J, Han P, Wang Y, Ye C, Weng D, Zhang F, Xu Z, Lei Y. 2016. DDX21 translocates from nucleus to cytoplasm and stimulates the innate immune response due to dengue virus infection. Biochem Biophys Res Commun 473:648-53.

69. Liu HM, Aizaki H, Choi KS, Machida K, Ou JJ, Lai MM. 2009. SYNCRIP (synaptotagmin-binding, cytoplasmic RNA-interacting protein) is a host factor involved in hepatitis C virus RNA replication. Virology 386:249-56.

70. Kim JH, Paek KY, Ha SH, Cho S, Choi K, Kim CS, Ryu SH, Jang SK. 2004. A cellular RNA-binding protein enhances internal ribosomal entry site-dependent translation through an interaction downstream of the hepatitis C virus polyprotein initiation codon. Mol Cell Biol 24:7878-90.

71. Balinsky CA, Schmeisser H, Ganesan S, Singh K, Pierson TC, Zoon KC. 2013. Nucleolin interacts with the dengue virus capsid protein and plays a role in formation of infectious virus particles. J Virol 87:13094-106.

72. Mihailovich M, Militti C, Gabaldón T, Gebauer F. 2010. Eukaryotic cold shock domain

proteins: highly versatile regulators of gene expression. Bioessays 32:109-18.

73. Phillips SL, Soderblom EJ, Bradrick SS, Garcia-Blanco MA. 2016. Identification of Proteins Bound to Dengue Viral RNA In Vivo Reveals New Host Proteins Important for Virus Replication. MBio 7:e01865-15.

74. Ju Lee H, Bartsch D, Xiao C, Guerrero S, Ahuja G, Schindler C, Moresco JJ, Yates JR, Gebauer F, Bazzi H, Dieterich C, Kurian L, Vilchez D. 2017. A post-transcriptional program coordinated by CSDE1 prevents intrinsic neural differentiation of human embryonic stem cells. Nat Commun 8:1456.

75. Hirano M, Muto M, Sakai M, Kondo H, Kobayashi S, Kariwa H, Yoshii K. 2017. Dendritic transport of tick-borne flavivirus RNA by neuronal granules affects development of neurological disease. Proc Natl Acad Sci U S A 114:9960-9965.

76. Larcher JC, Gasmi L, Viranaïcken W, Eddé B, Bernard R, Ginzburg I, Denoulet P. 2004. Ilf3 and NF90 associate with the axonal targeting element of Tau mRNA. FASEB J 18:1761-3.

77. Barber GN. 2009. The NFAR's (nuclear factors associated with dsRNA): evolutionarily conserved members of the dsRNA binding protein family. RNA Biol 6:35-9.

78. Gomila RC, Martin GW, Gehrke L. 2011. NF90 binds the dengue virus RNA 3' terminus and is a positive regulator of dengue virus replication. PLoS One 6:e16687.

79. Isken O, Baroth M, Grassmann CW, Weinlich S, Ostareck DH, Ostareck-Lederer A, Behrens SE. 2007. Nuclear factors are involved in hepatitis C virus RNA replication. RNA 13:1675-92.

80. Schumacher JM, Lee K, Edelhoff S, Braun RE. 1995. Spnr, a murine RNA-binding protein that is localized to cytoplasmic microtubules. J Cell Biol 129:1023-32.

81. Wolkowicz UM, Cook AG. 2012. NF45 dimerizes with NF90, Zfr and SPNR via a conserved domain that has a nucleotidyltransferase fold. Nucleic Acids Res 40:9356-68.

82. Salemi M, La Vignera S, Castiglione R, Condorelli RA, Cimino L, Bosco P, Romano C, Calogero AE. 2012. Expression of STRBP mRNA in patients with cryptorchidism and Down's syndrome. J Endocrinol Invest 35:5-7.

83. Pires-daSilva A, Nayernia K, Engel W, Torres M, Stoykova A, Chowdhury K, Gruss P. 2001. Mice deficient for spermatid perinuclear RNA-binding protein show neurologic, spermatogenic, and sperm morphological abnormalities. Dev Biol 233:319-28.

84. Shiina N, Nakayama K. 2014. RNA granule assembly and disassembly modulated by nuclear factor associated with double-stranded RNA 2 and nuclear factor 45. J Biol

Chem 289:21163-80.

85. El Fatimy R, Tremblay S, Dury AY, Solomon S, De Koninck P, Schrader JW, Khandjian EW. 2012. Fragile X mental retardation protein interacts with the RNA-binding protein Caprin1 in neuronal RiboNucleoProtein complexes [corrected]. PLoS One 7:e39338.

86. Anderson P, Kedersha N. 2006. RNA granules. J Cell Biol 172:803-8.

87. Bramham CR, Wells DG. 2007. Dendritic mRNA: transport, translation and function. Nat Rev Neurosci 8:776-89.

和文要旨

ダニ媒介性脳炎ウイルス(TBEV)はフラビウイルス属に分類され、人に重篤な脳炎を起こす人獣共通感染症の原因ウイルスである。自然界において、*Ixodes* 属のマダニと、げっ歯類を中心とした哺乳類動物の間で本ウイルスの感染環が成立している。ヒトは主に感染マダニの吸血によって TBEV に感染する。ヨーロッパ諸国とロシアを中心に年間約 10,000 人の患者が報告されているが、TBEV の病原性発現メカニズムはほとんど明らかになっておらず、未だ生ワクチンやウイルス特異的な治療法はない。また本ウイルスにはヨーロッパ型、シベリア型、極東型の 3 つのサブタイプが存在し、それぞれ異なる病態を示す他、同一のサブタイプにおいても株間で異なる病原性を有する株が報告されている。しかしそれらの病原性の相違を決定するウイルス側因子は、現在特定されていない。

第一章では、モンゴルにおける TBEV の疫学調査及び、分離されたウイルスの性状解析を行った。モンゴルでは過去に行われた調査においても、病原性の異なる 2 つのサブタイプが分布していることが示唆されているが、分離例も少なく病原性等の生物学的性状も不明である。そこで本研究では、モンゴル北部におけるダニ媒介性脳炎の疫学的危険度を評価するため、現在流行しているウイルスの分離及び生物学的性状の解析を試みた。モンゴル北部の Selenge 州において 26 プール（680 匹）の *I. persulcatus* 乳剤を接種した BHK 細胞において、9 プールが TBEV 遺伝子及びウイルス抗原陽性を示した。分離株のエンベロープ（E）タンパク質領域の遺伝子を解析したところ、全ての株が同一クラスターを形成し、シベリア型に分類されることが明らかとなった。このうち MGL-Selenge-13-12 および MGL-Selenge-13-14 の二株の分離ウイルスの全ゲノムを決定し、生

物性状解析を行ったところ、培養細胞においては同様の増殖性を示したが、マウスモデルにおいては異なる病原性を示した。全ゲノム解析から、この 2 株間では 13 個のアミノ酸の相違があり、これらの数個のアミノ酸自然変異が TBEV のマウスにおける病原性に関与していることが示唆された。

第 2 章では、低病原性を示す Oshima 5-10 株および、高病原性を示すロシアの脳炎患者由来である標準株の Sofjin-HO 株の病態発現機構における宿主との相互作用についての解析を試みた。TBEV の 3'-UTR variable region は株間での多様性が高く、ヒトの患者由来株や、実験室継代を繰り返した株においては、本領域における欠損や polyA の挿入が見られることが知られている。Oshima 5-10 株の 3'-UTR variable region 内には、7 つの stem loop (SL) 構造が存在することが知られており、このうち Sofjin-HO 株では 3、4 及び 5 番目の SL 構造（SL3、SL4 及び SL5）を欠損している。先行研究から、Oshima5-10 株の 3'-UTR variable region へ Sofjin-HO 株の 3'-UTR variable region を導入したウイルスでは、マウスにおける病原性が上昇する事が報告されている。このことから、ウイルス感染時における宿主応答が病態発現機構において役割を果たしていることが示唆された。本研究では、本領域と宿主との相互作用を調べるため、Oshima 5-10 株の 3'-UTR variable region に特異的に結合するタンパク質として CSDE1、FMRP、ILF3、STRBP を同定した。また、Sofjin-HO 株と同様の SL3-5 の欠損によっていずれのタンパク質との結合が減少し、SL 領域の部分的な欠損では宿主タンパク質との結合能が保持されることが示された。CSDE1 及び FMRP は RNA 代謝、ILF3 は免疫系の制御に関わる事が知られており、他のフラビウイルスの増幅においてもウイルス RNA と結合し作用することが報告されている。

以上の本研究結果から、TBEV の株間の病原性の相違は、ウイルス側因子の変化および宿主との相互作用が重要であることが明らかとなった。これら

の成績は、今後 TBEV をはじめとするフラビウイルスの病態発現機構の解明と、ワクチン及び予防・治療法の開発に大きく貢献するものと期待される。